Research Article

Annals of Dermatological Science (ISSN 2831-8129)

The mucocutaneous junction and its associated nerves, immunoreactive cells and changes with age: a review with novel observations from human fetal and cadaveric specimens.

Kei Kitamura[1†], Yuki Sugiyama[2†] , Kotoko Imai[2], Tianyi Yang[2], Ryo Sekiya[2], Kazuma Morita[2], Gen Murakami[2&3], Hitoshi Yamamoto[1], Shin-ichi Abe[2].

1. Department of Histology and Developmental Biology, Tokyo Dental College, Tokyo, Japan
   Email : keikitamura@tdc.ac.jp
   hyamamoto@tdc.ac.jp
   ORCID: 0000-0003-3335-1440
2. Department of Anatomy, Tokyo Dental College, Tokyo, Japan.
   Email : sugiyamayuki@jikei.ac.jp
   timaik@tdc.ac.jp
   yoteni@tdc.ac.jp
   sekiyaryo@tdc.ac.jp
   kmorita@tdc.ac.jp
   abesh@tdc.ac.jp
   ORCID: 0000-0003-4632-9736
3. Division of Internal Medicine, Iwamizawa Aska Hospital, Iwamizawa, Japan.
   Email : g.murakamisaori@gmail.com
   ORCID 0000-0001-7181-5475

† These authors contributed equally to this work

Corresponding author

Kitamura K, DDS, PhD ,
Department of Histology and Developmental Biology, Tokyo Dental College, Tokyo, Japan
Email : kitamurakei@tdc.ac.jp

Received Date : May 19, 2024
Accepted Date : May 20, 2024
Published Date : June 14, 2024

ABSTRACT

The mucocutaneous junction (MCJ) is a specific site located at body orifices such as the mouth, nose, eyelid, vulva, prepuce, and anus. The present study was conducted to reassess the MCJ in terms of 1) cytokeratin expression, 2) the distribution of immunoreactive cells, 3) nerves and their terminals, and 4) differences between near-term fetuses and adults. For cadaveric specimens after long-term preservation, cytokeratin 14 was useful for identification of the MCJ. In near-term fetuses, routine histology clearly demonstrated the putative MCJ due to transient, thick stratification of the squamous epithelium. This was most evident in the oral mucosa and less evident in the palpebral skin. In the anus and eyelid, the MCJ developed from highly proliferative epithelia of the anal sinus and meibomian gland, independent of the growing skin and mucosa. In elderly individuals, the MCJ was expanded in the nose and anus possibly as a result of mechanical stimuli, and was apparently connected to a hemorrhoid venous plexus. At the vulva and prepuce, a morphology intermediate between pseudostratified columnar and stratified squamous epithelia was evident. Except for the vulva and prepuce, corpuscle-like nerve terminals were sandwiched between the dermal papillae and epidermis, whereas nerves arranged in parallel exhibited free ends beneath the mucosa. At the anus, the myenteric autonomic nerve plexus disappeared slightly orad to the MCJ. Langerhans cells were richly distributed in the skin stratum spinosum, while suppressive T lymphocyte clusters were present in the lamina propria mucosae. General rules and site-specificity of the MCJ were reviewed.

Keywords

Mucocutaneous junction, lower lip, eyelid, external nasal orifice, vulva, prepuce, anus, immunohistochemistry, human fetus, elderly cadaver.

INTRODUCTION

The mucocutaneous junction (MCJ) is a specific site located at body orifices such as the mouth, nose, eyelid, vulva, prepuce, and anus. Classically, the MCJ epithelium was known to show desquamation with a lack of both desmosomal contact and a

Annals of Dermatological Science (ISSN 2831-8129)

lining of microplicae that anchor the polyanionic glycocalyx (e.g., [1]). Later, Knop et al. [2] and Tektaş et al. [3] newly defined the MCJ as having both para-keratinized cells ("pk cells" containing, but not totally filled with, bulky bundles of keratin filaments) and discontinuous para-keratinized epithelial cells. Thus, the concept of the MCL is essentially supported by electron microscopy observations. Conversely, however, identification of the MCJ was often difficult using routine histology, especially in human cadaveric specimens, due to delayed fixation or long-term preservation. Recently, in studies of nerves in the lip [4, 5], we have found that routine histology of specimens from near-term human fetuses can clearly demonstrate the MCJ (Fig. 1). This prompted us to attempt a comparison of skin and epithelial morphology in near-term fetuses.

Cytokeratin polypeptides (CKs) show organ-specific and epithelial type-specific expression (Table 1). The human skin epidermis strongly expresses CK1 and CK10 [6]. CK7 is a specific marker of the urogenital tract epithelium even in early fetal development [7, 8], although in larger fetuses the urogenital sinus-derived structure is positive for CK14 and CK17 rather than CK7 [9]. CK5 and CK6 (usually abbreviated as "CK5/6" because of the specificity of commercially-obtained antibodies) are used as markers of foregut-derived structures [10, 11]. Therefore, CK immunohistochemistry is a commonly accepted approach for studies of the MCJ [2, 3]. However, on sections from human cadaveric specimens, CK immunohistochemistry often yields poor results (inconsistent activity or loss) possibly due to delayed fixation or long-term preservation. On the basis of our previous studies using human cadaveric materials [12, 13, 14], we considered that a combination of CK5/6, CK14 and CK19 would be most useful. Langerhans cells (a type of dendritic cell), CD8-positive suppressor T-lymphocytes and macrophages are distributed in and/or beneath the epidermis and mucosal epithelium. However, it seems that few data are available regarding any changes in their distribution and density at the MCJ. Omine et al. [15] performed a limited study of differences in the density of these cells between the skin and mucosa at the eyelid, mouth, prepuce and anus (Table 2). Similarly, the distribution of free nerve terminals, especially those of pain nerves, and specific corpuscles and receptors has been described at limited sites, including the oral mucosa [16, 17], nasal respiratory epithelium [18, 19], glans penis [20, 21] and anus [22]. Conversely, few studies have demonstrated differences between the skin and the mucosa in the course (depth or lamination), density and terminal morphology of subcutaneous and submucosal nerves, except for the glans penis [23] and lower lip ([4], Table 3). Overall, in contrast to cytokeratin expression, there is little information about possible morphological changes in nerves and immunoreactive cells at the MCJ.

In the present study, on the basis of our previous studies as well as some new histological findings, we aimed to clarify histological changes at the MCJ in terms of 1) cytokeratin expression, 2) the distribution of Langerhans cells and other immunoreactive cells, 3) the course of nerves and terminals beneath the epithelium, and 4) transient morphologic changes in fetuses and suggested degenerative features associated with age.

MATERIALS AND METHODS

This study was conducted in accordance with the provisions of the Declaration of Helsinki 1995 (as revised in 2013). Reviewed descriptions were based on our previous studies of the eyelids [5, 15, 24, 25], the lip and mouth [4, 15, 26], muscles at the nasal orifice [27, 28, 29], the glans penis [15, 23], the vulva [30] and the anus [31, 32, 33, 34, 35]. Because the MCJ was not the focus of these previous studies, however, we re-examined sections that had been prepared at the time and, at some sites, we conducted additional immunohistochemistry using unstained sections (for methods, see the final subsection of Materials and Methods).

Furthermore, based on observations of newly-prepared histological sections from eight adult cadavers and seven human fetuses (for details, see the subsections below), a number of novel descriptions were also included in the present study.

Adult cadaveric specimens

We dissected eight cadavers (three men and five women; aged 78–96 yr) that had been donated to Tokyo Dental College, Tokyo, Japan, for research and education on human anatomy with the approval of the Tokyo Dental College committee for research use (No. 922-2). These cadavers had been fixed by arterial injection of 10% neutral aqueous formalin solution and stored in 50% ethanol for more than 3 months. The external nose including the deep mucosa as well as the vulva including the distal urethra were removed from the cadavers and, using tissue blocks, routine procedures for paraffin-embedded histology were performed. Most sections were stained with hematoxylin-eosin (HE), azan, Masson trichrome or elastica Masson, while a smaller proportion was used for immunohistochemistry (see the final paragraph below). With elastica Masson staining (a variation of Masson-Goldner staining [36, 37]), elastic fibers are stained black, collagenous fibers appear green and striated muscles are bright red. All photographs were taken with a Nikon Eclipse 80.

Human fetus specimens

The seven late-stage fetuses were part of the collection kept at

Annals of Dermatological Science (ISSN 2831-8129)

the Department of Anatomy, Akita University, Akita, Japan. They had been donated by the families concerned to the Department in 1975–1985 and preserved in 10% w/w neutral formalin solution for more than 30 years. Data for these specimens included the date of donation and the number of gestational weeks, but did not include the name of the family, obstetrician or hospital, or the reason for abortion. The use of these specimens for research was approved by the Akita University Ethics Committee (No. 1428) and the sixth author (G.M.) is one of members of the research project. The research ethics committee of Tokyo Dental College also approved the use of the materials (No.932-2). The whole head of each fetus was obtained after removal of the brain and cutting below the hyoid bone as well as the pelvic region below the iliac crest, and after cutting at the midportion of thigh. Before routine procedures for paraffin embedding, the head and pelvic tissue masses were decalcified by incubating them at room temperature in Plank-Rychlo solution (AlCl2/6H2O, 7.0 w/v%; HCl, 3.6; HCOOH, 4.6) for 3-7 days. The sectional planes were sagittal (2 specimens), frontal (3) or horizontal (2). Most sections were stained with (HE), azan or Masson trichrome, while a minor part was used for immunohistochemistry (see below the final paragraph). All photographs were taken with a Nikon Eclipse 80.

Immunohistochemistry of fetal and elderly adult specimens

The primary antibodies used were 1) rabbit polyclonal antibody for S100A1 protein (Dako Z0311; Dako, Glostrup, Denmark), 2) mouse monoclonal antibody for vasoactive intestinal polypeptide (VIP) (sc25347; Santa Cruz; Santa Cruz, CA, USA), 3) mouse monoclonal antibody for cytokeratin-19 (sc-6278; Santa Cruz), 4) mouse monoclonal antibody for cytokeratin-14 (LL002; Novocastra, Newcastle upon Tyne, UK), 5) mouse monoclonal antibody for cytokeratin 5/6 (M7237, Dako), 6) mouse monoclonal antibody for CD1a (M357101-2, Dako), 7) mouse monoclonal antibody for CD8 (N1592, Dako) and, 8) mouse monoclonal antibody for chromogranin A (M0869, Dako). 9) mouse monoclonal antibody for alpha smooth muscle (M0851, Dako). For cytokeratin and CD-family antigens, antigen retrieval was performed with microwave treatment (500W, 15 min, pH 6). The secondary antibody (incubation for 30 min; dilution 1:1000; Histofine Simple Stain Max-PO, Nichirei, Tokyo) was labeled with horseradish peroxidase (HRP), and antigen-antibody reactions were detected using diaminobenzidine as the chromogen (incubation for 3-5 min; Histofine Simple Stain DAB, Nichirei, Tokyo). All samples were counterstained with hematoxylin. Negative controls consisted of samples without primary antibody.

RESULTS

Data from references and our previous studies are summarized in four tables: cytokeratin expression (Table 1), immunoreactive cell distribution (Table 2), nerve course and terminal morphology beneath the skin-MCJ-mucosa (Table 3), and distinct changes with age in the surface histology and composite cells (Table 4). These tables overlap the text descriptions below somewhat, and sometimes differ from our novel findings reported here. To address these differences, the reader is directed to "See also the subsection entitled XX in the Results" in the table footnotes. When references are limited in number, especially for the nose and genitalia, appropriate newly-taken photos are provided (i.e., Figs. 1, 4, 5, 8 and 9).

Table 1. Expression of cytokeratin polypeptides (CK) in the skin, mucosaand MCJ.

	Skin	MCJ	mucosa
Lip[1)]	CK1,10-positive	CK14-positive	CK14,19-positive
Nose[2)]	CK13-positive	CK13-positive	CK13-negative
Eyelid[3)]	CK10-positive	CK10-positive, CK19-negative	CK13,19-positive
Urethra[4)]	CK10-positve	CK7-positive, CK10-negative	CK7-positive
Anus[5)]	CK5,10,13-positive	CK19-positive	CK8,18,19-positve

References: 1) Barret et al. [60](see also a subsection entitled "Lips and mouth" in the Results); 2) Kasper et al. [61], Schwerer et al. [62]. See also a subsection entitled "Nasal orifice" in the Results. 3) Tektaş et al. [3]. 4) Herrera-Imbroda et al. [7], Shen et al. [8]. 5) Levy et al. [63], Williams et al.[64]

Annals of Dermatological Science (ISSN 2831-8129)

Table 2. Langerhans' cell and other immunoreactive cells in the skin, mucosa and MCJ

	Skin	MCJ	mucosa
Lip[1)]	Langerhans+ CD8+ >or< CD4? DC+	no distinct change	Langerhans++ CD8+ > CD4 DC+
Nose[2)]	Langerhans+	MCJ-M, gradual change Langerhans absent	Langerhans+or CD4+ > CD8+ DC+
Eyelid[3)]	Langerhans++	gradual change	Langerhans+ CD8+ > CD4+ CD8+ in epithelium; CD4+ in lamina propria
Vulva, prepuce[4)]	Langerhans+	gradual change	Langerhans-
Anus[5)]	Langerhans++ CD8+ > CD4+	MCJ-M, drastic change Langerhans+	Langerhans CD8+ > CD4+ DC+

DC, non-Langerhans type dendritic cells such as CD209 (DC-SIGN)-positive cells.

References:

1) Mechtersheimer et al. [65], Cruchley et al. [66], Omine et al. [15], Reinartz et al. [67].

2) Yoshimi et al. [68], Graeme-Cook et al. [69], Kawahara et al. [59], Takasaki [70], Jahnsen et al. [40], Morinaka et al. [71], Jahnsen et al. [41], Karosi et al., 2013. See also a subsection entitled "Nasal orifice" in the Results.

3) Hingorani et al. [73], Omine et al. [15].

4) Morelli et al. [74], Omine et al. [15], Qin et al. [75].

5) Mechtersheimer et al. [65], Gervaz et al. [76], Omine et al. [15].

Table 3. Nerve course and terminal morphology in the skin, mucosa and MCJ

	Skin	mucosa	MCJ
Lip1)	corpuscle-like terminal along the dermal papilla	free end of twigs parallel to surface Merkel-neurite complex absent varicose-like structure, mechanoreceptors	drastic change
Nose2)	free end substance P+ nerve	free end substance P+ nerve other peptidergic nerves	distinct change to M free end?
Eyelids3)	corpuscle-like terminal, free nerves parallel to epithelium	free end	distinct change to M corpuscle-like terminal
Vulva, prepuce4)	free end dominant Meissner's corpuscles	free end	distinct change in density
Anus5)	free end	Myenteric plexus abundant ganglia	gradual but distinct change free end, a few ganglia Pacinian corpuscle

References: 1) Ramieri et al. [16], Hilliges et al. [77], Watanabe [17], Cho et al. [5]. 2) Lundblad et al. [18], Zhao et al. [78], Hauser-Kronberger et al. [19]. See also a subsection entitled "Eyelids" in the Results. 3) Cho et al. [4].

4) Halata et al. [20], Hinata et al. [79], Kurokawa et al. [30], Jang et al. [23], García-Mesa et al. [21]. 5) Li et al. [22], Hieda et al. [33], Ishiyama et al. [34], kinugasa et al. [35].

Table 4. Distinct changes with age in the surface histology and composite cells

	Skin	mucosa	MCJ
Lip[1)]		lost cornification[6)]	difference in nerve course[8)]
Nose[2)]	lost cornification		elongation
Eyelids[3)]		lost stratification after birth[7)]	some nerves disappear[9)]
Vulva, prepuce[4)]	lost cornification		pseudostratified to squamous
Anus[5)]	lost cornification		elongation with fetus anal sinuses involved immunoreactive cell infiltration, venous plexus proliferation

References: 1) Cho et al. [5]. 2) See also a subsection entitled "Nasal orifice" in the Results. 3) Cho et al. [4]. 4) See also a subsection entitled "Vulva and prepuce" in the Results. 5) See also a subsection entitled "Anal canal" in the Results. 6) Lost cornification: the cornification corresponds to a highly increased stratification with hypertrophied keratinized cells (Kim et al. [14]). A transient closure of the lumen is evident in the external auditory meatus and nasal orifice (Fig. 3i) and also seen at the anus and male urethral orifice (Fig. 9C). 7) In fetuses, the conjunctival epithelium is stratified cuboidal, not simple cuboidal. 8) A sudden change in nerve course and terminal at the MCJ of lips becomes evident possibly after birth (Cho et al. [4]). 9) Subepithelial nerve twigs in parallel to the MCJ epithelium of eyelids were seen in fetuses (Cho et al. [5]), but they were not reported in adults

Lips and mouth

The lips showed the typical changes in MCJ morphology immediately outside or anterior to the approximation surface (free surfaces attached to each other between the upper and lower lips). Thus, the approximation surface corresponded to the mucosa. The change was marked at near-term because, in the mucosa with hypertrophic surface cells, the stratification was 6-7 times taller or thicker than that of the skin (Figs. 1j and 2h).

According to Cho et al. [4] and our re-examination for the present study, the lip skin epidermis in elderly individuals expressed cytokeratin-14 (CK14) at any depth, while CK14 positivity was limited to the most superficial lamina of the stratified epithelium of the mucosa and MCJ (Fig. 2cd). Thus, the lip skin exhibited sudden loss of strong CK14 positivity at the MCJ. CK5/6 and CK19 were negative in three parts of the lip in elderly individuals. However, these results differ from those in the references (Table 1). Langerhans cells were richly distributed in the stratum spinosum, while CD8-positive T lymphocytes were dominant in the lamina propria beneath the mucosal epithelium (Fig. 3). In the elderly, the lip mucosa lacked a tall stratified layer, often resembling simple squamous epithelium (Fig. 2a).

Near the free margin of the lower lip, a thick branch of the mental nerve turned superficially (anteriorly) to pass through the upper end of the orbicularis muscle layer to supply the lip skin, whereas another thick branch took a reverse J-shaped course along the stratified squamous epithelium of the free margin and reached the MCJ. In the subcutaneous tissue, nerve twigs were concentrated along and around veins and dermal papillae. At the MCJ, terminal nerve twigs running in parallel to the mucosal surface were replaced by capsule-like nerve terminals attached to or surrounding internal protrusions of the skin stratum spinosum between the dermal papillae. This change in nerve terminals was much more evident in elderly individuals than in fetuses (Fig. 2e-g).

Overall, in the fetal lips, the mucosa was characterized by 1) very thick stratification of the cornified layer and 2) a short and abrupt change at the MCJ where thick cornification was lacking (Table 5). As nerve twigs are likely to be underdeveloped even in late-stage fetuses, a drastic change in nerve terminals at the MCJ would likely occur after birth or when suckling is initiated.

Annals of Dermatological Science (ISSN 2831-8129)

Table 5. Site-specific morphologies of the skin-MCJ-mucosa in fetuses

	Skin	MCJ area	mucosa
Lip[1)]	hairs	short & sudden change	very thick stratification
Nose	hairs; striated muscle insertion to the dermis	long and wide, but drastic at MCJ-Mucosa, extending with age	columnar with cilia
Eyelids[2)]	eyelash; Skin-MCJ, a small difference in stratification	MG duct opening	cuboidal with vacuole
Vulva, prepuce[3)]	thick stratification, no hairs, no dermal papillae	long and wide similar to stratified squamous cavernous sinus & smooth muscle	pseudostratified pale-colored tall cells
Anus[4)]	abundant small dermal papillae no hairs facing the lumen	long and wide, but drastic at MCJ-Mucosa dilated veins	columnar with goblet cells

1)In the lips, lost thick stratification of the oral mucosa seemed to occur after birth: but this change seemed not to induce an internal extension of the skin.

2) Meibomian gland (MG) epithelium is similar to and continues to the MCJ.

3) In the vulva and prepuce, a long and wide MCJ (possibly underdeveloped pseudostratified but similar to the stratified squamous) seems to be maintained after birth.

4) The anal transitional zone epithelium initially develops as the fetal anal sinus that widen a circumference of the anal canal prenatally. Thus, the anal "MCJ" in adults does not develop as a junction between the skin and mucosa but as an independent epithelium derived from a secondarily-added structure.

Nasal orifice

The nasal mucosa is a pseudostratified columnar epithelium with cilia (Figs. 1k, 4ch and 5ek), although the cilia were usually damaged due to long lag-time after death in the present materials. The MCJ was short and composed of a thin stratified squamous epithelium at near-term and with few goblet cells in elderly individuals (Figs. 1g, 4d and 5d). The skin was very long and wide in the elderly and often reached a depth of more than 30 mm within the orifice (e.g., almost 20 mm in Fig. 5). The MCJ was usually lower or more superficial in the medial (septal) side than the lateral (alar) side. The nasal skin was characterized by striated muscle fibers contained; near-term specimens clearly demonstrated nasalis muscle fibers passing between the glands or hairs and inserting deeply to the dermis (Fig. 4). In fetuses at 10-16 weeks, the nasal orifice was transiently closed by cornification or hypertrophic keratinized cells [14] (Fig. 3i). The nasal MCJ, as thick as the nasal skin epidermis, had no or few internal protrusions of the stratum spinosum (or the corresponding dermal papillae) and lacked hairs and nasalis muscle. Instead, a vein-rich, loose tissue was present beneath the MCJ.

Cytokeratin-13 is positive in the skin as well as the MVJ but negative in the nasal mucosa (Table 1). We observed that cytokeratin-14 reactivity was strong on the basal side of the epidermis, weak at the MCJ, and very weak in the mucosal epithelium (Fig. 5c-e). Acinus cells beneath the mucosa were positive for cytokeratin-14. Nerves were few beneath the MCJ and mucosa (Fig. 4h). However, in the subcutaneous tissue, abundant nerves took wavy courses while maintaining an almost constant depth of 1 mm beneath the epidermis (Fig. 4g). Thus, the skin nerves crossed striated muscle fibers at almost right angles. Langerhans cells were rich in the skin epidermis, especially in and along hair follicles, but absent at the MCJ and in the mucosa (Fig. 5f-h). In the mucosa, it had been reported that CD4-positive T lymphocytes were more dominant than CD8-positive cells. However, we found only a few CD4-positive T lymphocytes at all sites near the nasal orifice. Mononuclear cells including CD8-positive T lymphocytes had infiltrated beneath the epidermis and MCJ, but were absent in the mucosa (Fig. 5i-k). Notably, CD8-positive cells were seen in both the epidermis and columnar epithelium (Fig. 5i and k). These lymphatic tissues appeared not to correspond to the nasal-associated lymphoid tissue (NALT) that has been defined in animals. To our knowledge, studies of human NALT have not focused on areas at and near the MCJ but rather deep areas near the pharyngeal and tubal tonsils [38, 39]. The human NALT contains not only subtypes of macrophage and dendritic cells but also M cells [40, 41]. Overall, at the nasal orifice, the skin was characterized by striated muscle fibers inserting to the dermis. CD8-positive cells were present in both the epidermis and columnar epithelium. After birth, the MCJ is most likely to expand deeply (posteriorly and superiorly). Therefore, a deep and abrupt change between the MCJ and ciliated mucosa was often evident in aged individuals (Table 5).

Annals of Dermatological Science (ISSN 2831-8129)

Eyelids

The morphology of the eyelid MCJ has been described in detail by European groups (see the Introduction). In short, the epithelium has been characterized by "para"-keratinization and discontinuity, and subsequently the MCJ was reported to correspond to the posterior or internal 1/3 of the approximation surfaces between the upper and lower lids. Thick ducts of meibomian glands opened to the MCJ and the duct epithelium appeared to supply epithelial cells to the MCJ. Riolan's muscle (striated muscle; the inferoposterior end of the orbicularis oculi muscle) was located close to the MCJ epithelium. The duct was always dilated at near-term (Fig. 6a) because the opening was obliterated, possibly due to high cell proliferation rate of the MCJ.

The palpebral skin and MCJ were cytokeratin10 (CK10)-positive, while the conjunctival mucosa was cytokeratin19-positive (Table 1). In near-term fetuses, the approximation surfaces of the eyelids contained abundant corpuscle-like nerve terminals at the base of the epithelium. Simultaneously, the lamina propria contained nerve twigs running in parallel to the epithelium (Fig. 7d). However, the parallel nerves are likely to be restricted beneath the approximation surface [5] (Fig. 7c). Langerhans cells were rich in the skin and MCJ and few in the mucosa. CD8-positive T lymphocytes were dominant beneath the epithelium at any site and depth (Table 2; Fig. 7ef). In elderly individuals, the entire approximation surface appeared to carry thick stratified squamous epithelium, but contained surprisingly few nerves.

The surface morphologies in Fig 1chl (252 mm CRL) are quite different from those in Fig. 6 (270 mm CRL). The former (252 mm) upper lid, possibly poorly differentiated, carries a thin epidermis of palpebral skin, thick stratification at the approximation surface, and the cuboidal epithelium of the conjunctiva. The latter (270 mm) is well differentiated and shows thick epidermal stratification (Fig. 6b), thin stratification of the approximation surface, and pseudo-stratified cuboidal epithelium of the conjunctiva (Fig. 6fk). The specific cuboidal epithelium contains vacuoles in the surface cells of the lower palpebral conjunctiva. The cells with vacuoles were considered likely to develop to goblet cells [42, 43]. In these large fetuses, it was rather easy to discriminate the "approximation surface epithelium" (not the MCJ) from either the skin or the mucosa. The typical MCJ as defined by European groups (see above) might be established after birth.

Overall, in the fetal eyelids, any difference between the MCJ and thin palpebral skin was limited: 1) eyelashes and slightly thicker stratification in the skin and 2) meibomian duct epithelium continuous with the MCJ with obliterated ductal openings. Similarly, a gradual change between the MCJ and conjunctiva was characterized by candidate goblet cells and intercellular slits in the cuboidal mucosal epithelium (Table 5). Thick stratification is not evident in the eyelids, especially at the approximation surface.

Vulva and prepuce

In 10-15 weeks at midterm, the epidermis showed a marked increase of stratification thickness at the deep skin groove of the vulva (Fig. 8b) and the skin surrounding the space between the prepuce and the glans penis (Fig. 9bc). The latter space around the glans was filled and obliterated with cornification (Fig. 9c) and epithelial pearl-like structures were present (Fig. 9b). Epithelial pearls are a well-known feature of the oral mucosa, especially in the palatal aspect [27].

The MCJ epithelium at the urethral orifice changes abruptly to a thin stratified squamous epithelium (Figs. 1i and 8egh) and continued to the pseudostratified columnar epithelium of the distal urethra (Figs. 1m, 8i, 9d and 10d). The squamous MCJ of the vulva was also connected to the highly stratified epithelium of the vagina (Fig. 8d). In adults, the vulva and glans penis are covered by a specifically thin epidermis without a lining of dermal papillae. The subcutaneous tissue contained a complex of cavernous venous sinuses (Figs. 8gh and 10a).

Beneath the skin, nerve density in the vulva was much lower than in the prepuce (Fig. 8j vs. Fig. 10c), and corpuscle-like nerve terminals were considered to be likely absent in females (Table 3). The skin of both the vulva and prepuce was CK10-positive, while the MCJ and urethral mucosa were CK7-positive even in early fetuses. Langerhans' cells were seen in the skin and MCJ, and CD8-positive T lymphocytes were richly present at any site and depth (Fig. 10ef). According to our interpretation of [44], the genital MCJ was considered likely to contain immunoreactive cells similar to those in the nasal MCJ in terms of density and subtype. The tunica albuginea enclosed the corpus cavernosus penis even in fetuses (Fig. 9a), but we found no evidence for blending of the tunica with the dermal papilla at sites distant from the glans as reported by Halata and Munger [20].

Overall, in both fetal and cadaveric specimens, the prepuce and vulva were characterized by 1) a lack of hairs and dermal papillae, 2) a long and wide MCJ with a specific surface, and 3) a cavernous sinus of veins and smooth muscles distributed beneath the skin and MCJ. The specific surface was covered by apparently underdeveloped pseudostratified columnar epithelium, although there was some resemblance to stratified squamous epithelium. As was evident in the urethra of elderly individuals, the MCJ in young adults might possess true pseudostratified epithelium comprising pale-colored tall cells (Table 5).

Annals of Dermatological Science (ISSN 2831-8129)

Anal canal

The anal skin had tall stratified layer at midterm (Figs. 1e and 11ef), but this was lost at near-term. Conversely, the columnar epithelium became tall until near-term. From the rectal side to the skin side, the anal canal epithelium changed from columnar epithelium with abundant goblet cells (Fig. 11b), via cuboidal epithelium with few goblet cells (anal transitional zone=MCJ; Figs. 1n and 11c), to stratified squamous epithelium (anal skin; Figs. 1e and 11d). Being independent of both the squamous skin and columnar mucosa, the putative MCJ initially developed as an epithelium of the anal sinuses that considerably increased the circumference of the anal canal at midterm [32](Fig. 11f). The MCJ expresses SOX2 but the anal skin and mucosa do not [45].

The anal canal possessed a muscularis mucosae or anal submucosal smooth muscle (Figs. 11a and 12ad) between the mucosal epithelium and circular muscle layer (the latter representing the internal anal sphincter), but the submucosal muscle showed great individual variations in thickness and extent [31]. Beneath the MCJ, the submucosal muscle fibers disperse and disappear (Fig. 12e).

The myenteric or intermuscular autonomic nerve plexus disappeared slightly orad to the MCJ (Fig. 11e). Thus, the skin side of the mucosa did not carry the nerve plexus, but ganglion cell clusters were sparsely distributed in the intersphincteric zone beneath the MCJ. Notably, submucosal nerve twigs are few or even absent beneath the MCJ in contrast to abundant nerves beneath the skin and mucosa (Fig. 12b). Conversely, chromogranin-positive neuroendocrine cells are few in the mucosa (Fig. 12f), absent in the skin (Fig. 12c) and rich at the basal layer of the MCJ (Fig. 12g). Hörsch et al. [46, 47] demonstrated chromogranin-positive elongated neuroendocrine cells distributing densely at the anal MCJ. Some of neuroendocrine tumors from the anal canal also express chromogranin A [48, 49].

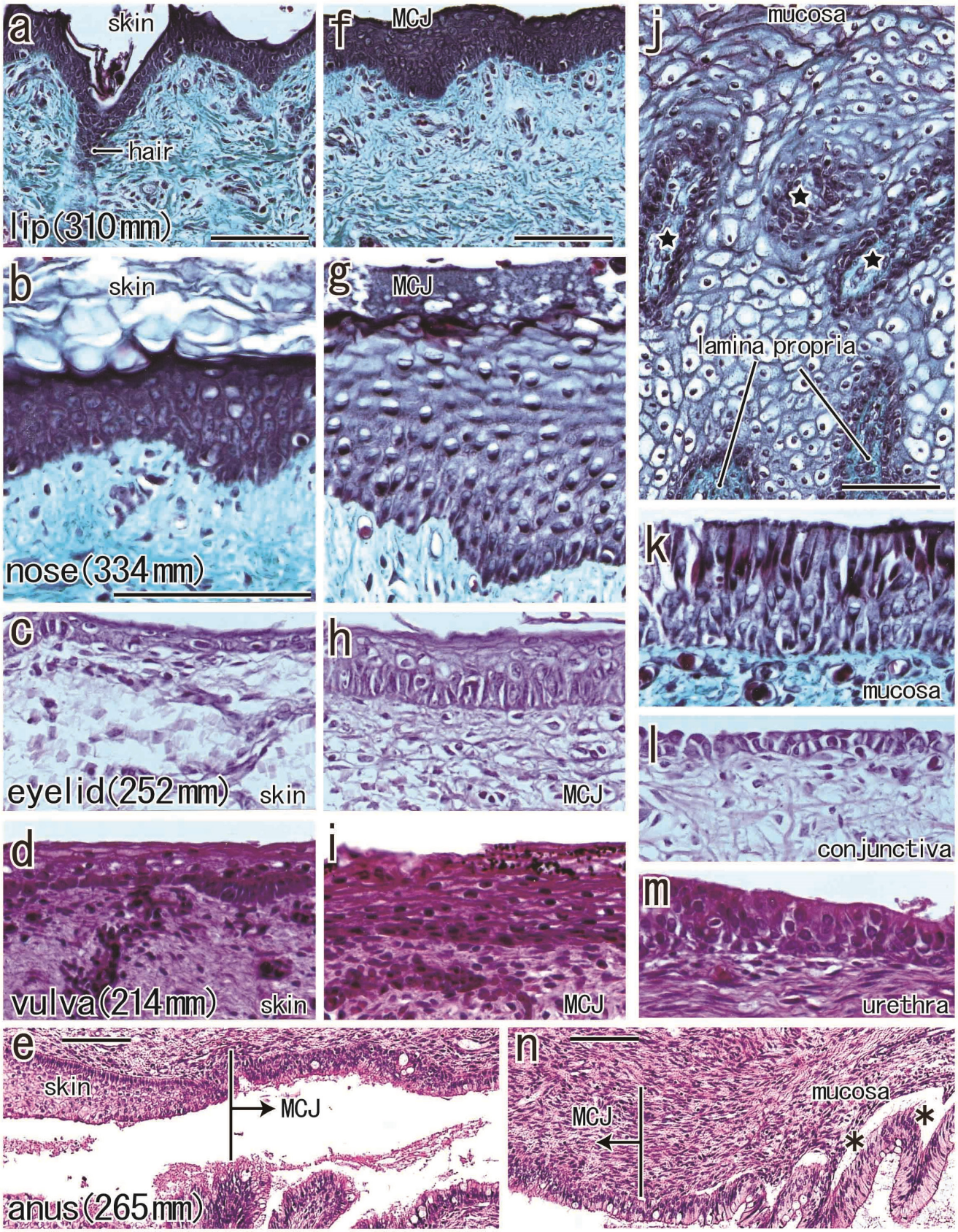
In elderly individuals, the MCJ was characterized by infiltration of lymphocytes and macrophages and, beneath it, dilated hemorrhoidal veins were evident (Fig. 11ac). Langerhans cells were more numerous than CD8-positive lymphocytes in the anal skin and MCJ (two inserts in Fig. 11a).

Overall, in the fetal anal canal, the skin was characterized by 1) a lack of hairs facing the lumen and 2) abundant small dermal papillae. The MCJ is derived from the fetal anal sinus epithelium, being analogous to the eyelid MCJ derived from the meibomian duct. Anal glands are open to the anal MCJ [45, 50], but the ducts are underdeveloped in fetuses. The long and wide MCJ observed in elderly individuals had accompanying well-developed venous plexuses and mononuclear cell infiltration. The anal MCJ is known to be a site where composite lymphoid tissues undergo a suppressive reaction under conditions of virus infection [50, 51]. Finally, intestinal nerve plexuses never extended to the MCJ (Table 5).

Annals of Dermatological Science (ISSN 2831-8129)

FIGURES

Figure 1. Mucocutaneous junction in near-term fetuses.

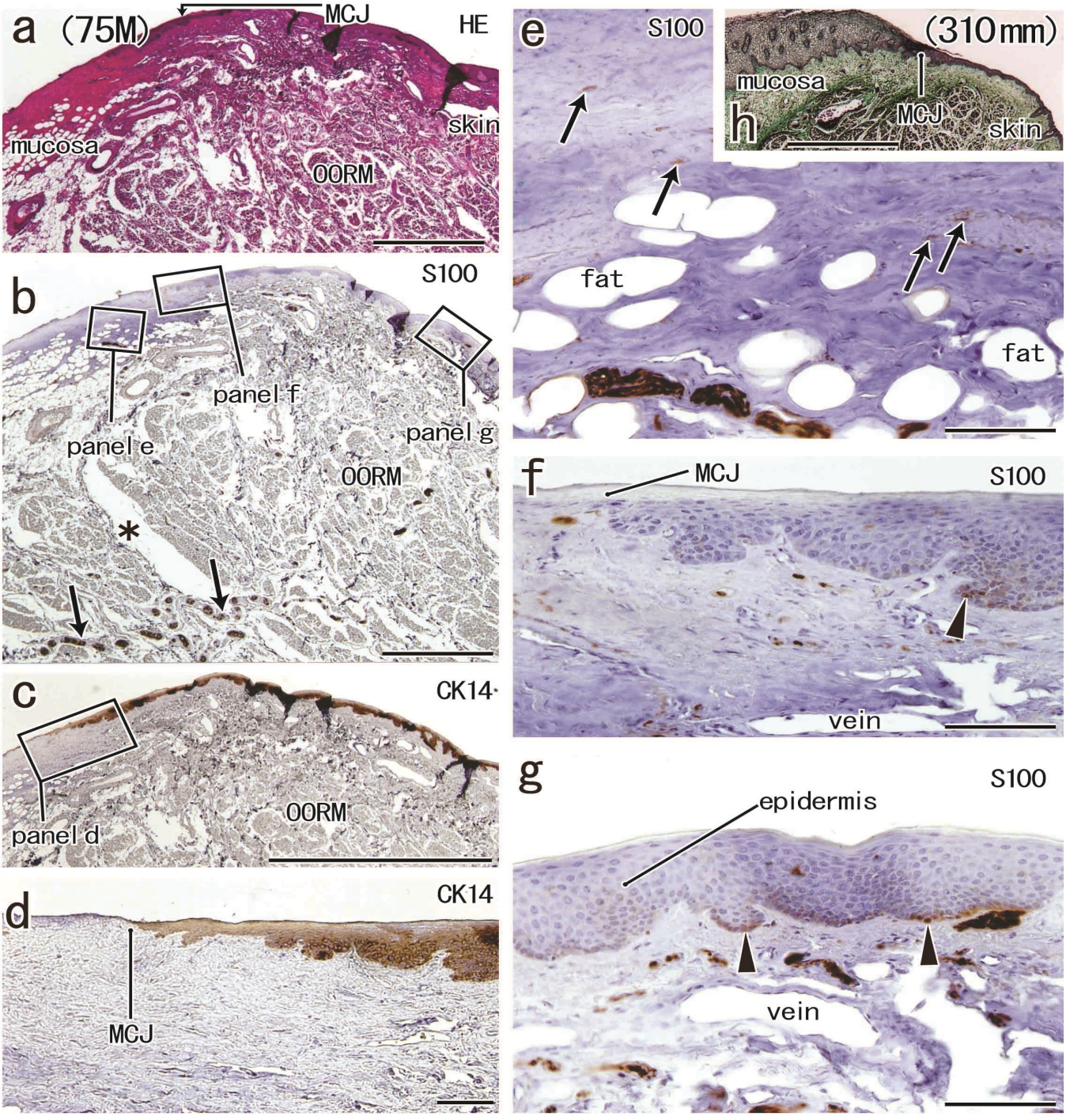


The middle column of panels shows the mucocutaneous junction (MCJ). Panels a, f and j (Masson trichrome), lower lip of a 310-mm fetus; panels b, g and k (Masson trichrome), external nasal orifice of a 334-mm fetus; panels c, h and l (HE), upper eyelid and palpebral conjunctiva

Annals of Dermatological Science (ISSN 2831-8129)

of a 252-mm fetus; panels d, i and m (HE), vulva and female urethra of a 214-mm fetus; panels e and n (HE), anal canal of a 265-mm fetus. In the lower lip (panels a, f and j), note very tall stratified squamous epithelium with protrusions of the lamina propria mucosae (stars in panel j). Panel k displays ciliated pseudostratified columnar epithelium (respiratory epithelium) of the nose. In the upper eyelid, the MCJ morphology (panel h) is seen at the approximation surface in near-term fetuses. The distal female urethra (panel m) carries pseudostratified columnar-like epithelium at near-term: it is also similar to transitional epithelium in the male urethra. Tall stratification of the anal skin (panel e) is lost and goblet cells (arrows) appear in the MCJ of the anus (panel e) and, then, the latter changes into the columnar epithelium (panel n). Asterisks in panel n indicate an artifact separation of the mucosa. Lower-magnification views are shown in Fig. 2h (lip), Fig. 4e (nose), Fig. 6a (eyelid), Fig. 8c (vulva) and Figs. 11ef and 12ac (anus). Panels a, f and j or panels b-d, g-i ,k-m and e and n were prepared at the same magnification (scale bars: 0.1 mm in panels a, b, e, f, j, n; 0.5 mm in panel e; 5 mm in panel n).

Figure 2. Nerve distribution in the lower lip of a 75-year-old man: immunohistochemistry for S100 protein and cytokeratin 14 at the MCJ.

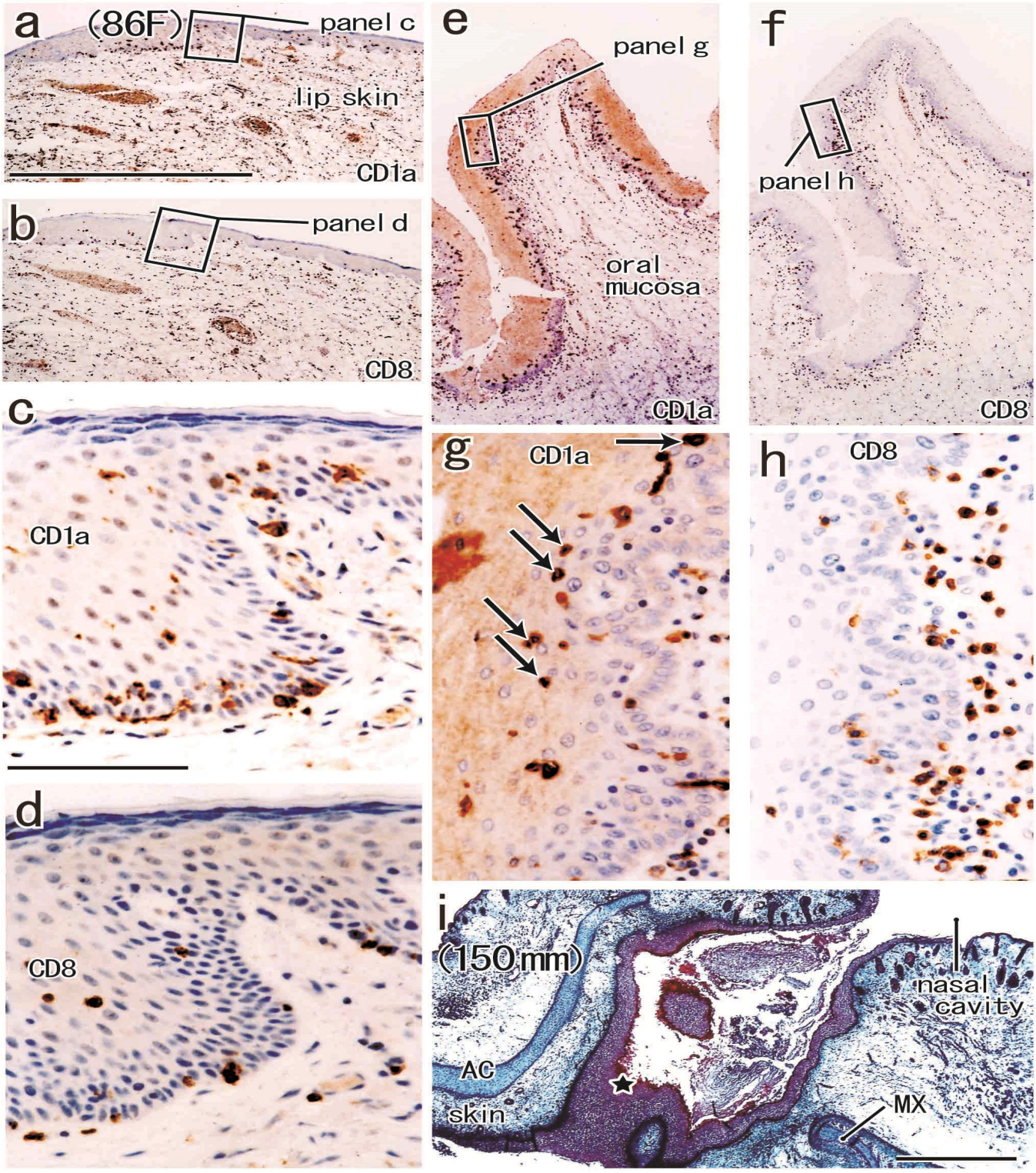


Sagittal sections. HE staining (panel a); immunohistochemistry for S100 protein (panels b and e-g); immunohistochemistry for cytokeratin-14

Annals of Dermatological Science (ISSN 2831-8129)

(panels c and d). Higher-magnification views of the squares in panel b (or panel c) are shown in panels e-g (or panel d). Panels a-c show adjacent sections. Thick nerve branches run anteriorly through the orbicularis oris muscle layer (OORM) toward the skin side of the lower lip (panel b). The stratum spinosum of the epidermis is strongly positive for cytokeratin 14 (CK14; panels c and d), in contrast to the mucosa. At the MCJ (panel f), the epidermis appears abruptly. The mucosa contains thin nerve twigs (arrows in panel e), while the stratum spinosum contains corpuscle-like nerve terminals at the base facing the dermal papillae (arrowheads in panels f and g). Panel h shows the near-term lip: the MCJ is clear because of the very thick stratified epithelium of the mucosa (see also Fig. 1j). Scale bars, 1 mm in panels a-c and h; 0.1 mm in panels d-g.

Figure 3. Immunoreactive cells in the oral mucosa and lower lip skin from an 86-year-old woman.

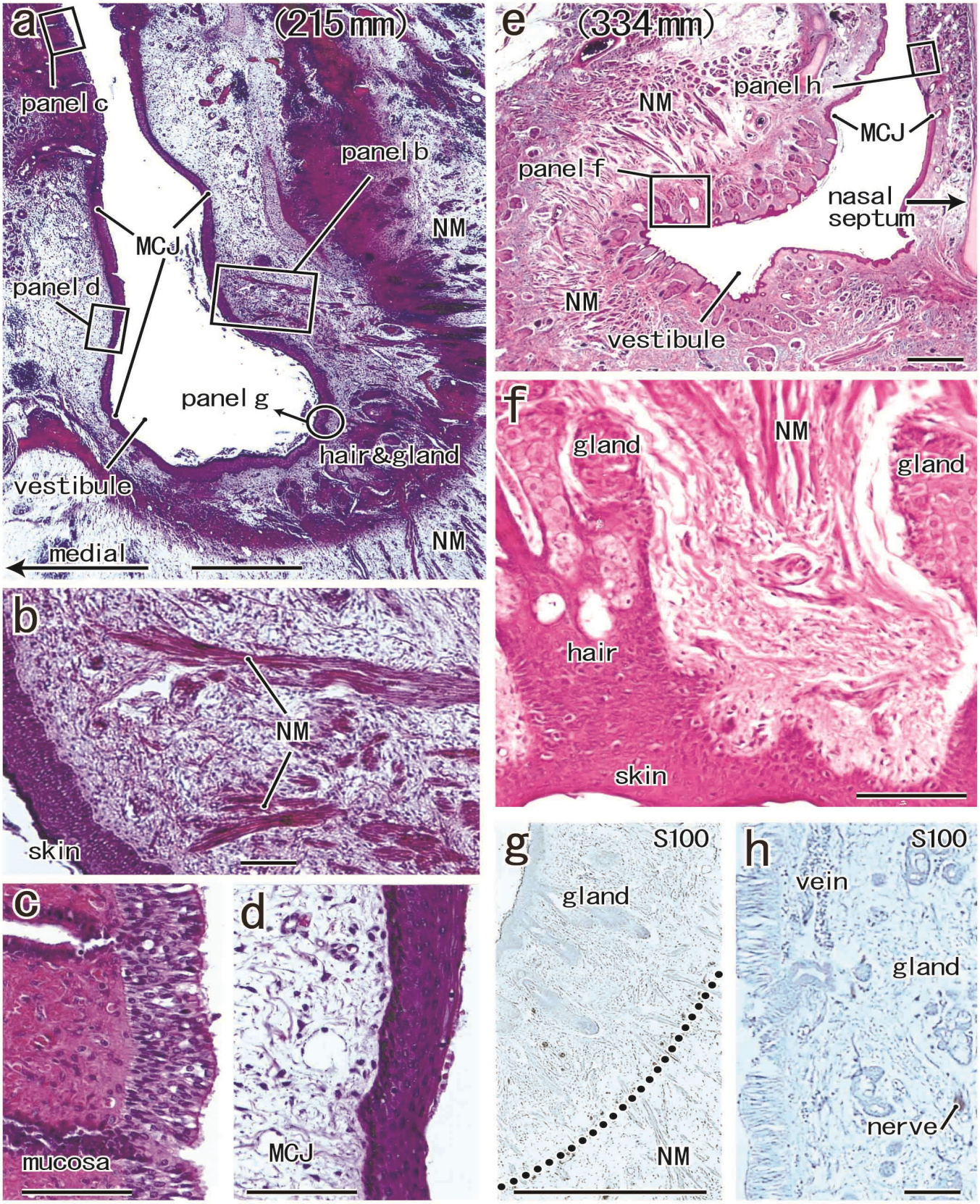


Panels a-d display the lower lip skin, while panels e-h show the oral mucosa near the lower lip. Panels c and d (or panels g and h) are higher-magnification views of the squares in panels a and b (or panels e and f), respectively. The stratum spinosum of the lip skin contains abundant

Annals of Dermatological Science (ISSN 2831-8129)

CD1-positive Langerhans cells (panel c) and a few T-lymphocytes (panel d). The oral stratified epithelium contains abundant Langerhans cells (arrows in panel g), while T-lymphocytes are restricted to the submucosal side of the mucosa (panel h). Panel i shows a sagittal section (elastica Masson staining) of the nasal orifice of a 150-mm fetus and a star indicates cornification closing the orifice. AC, alar cartilage; MX, maxilla. Panels a, b, e and f or panels c, d, g and h were prepared at the same magnification (scale bars: 1 mm in panels a and i; 0.1 mm in panel c).

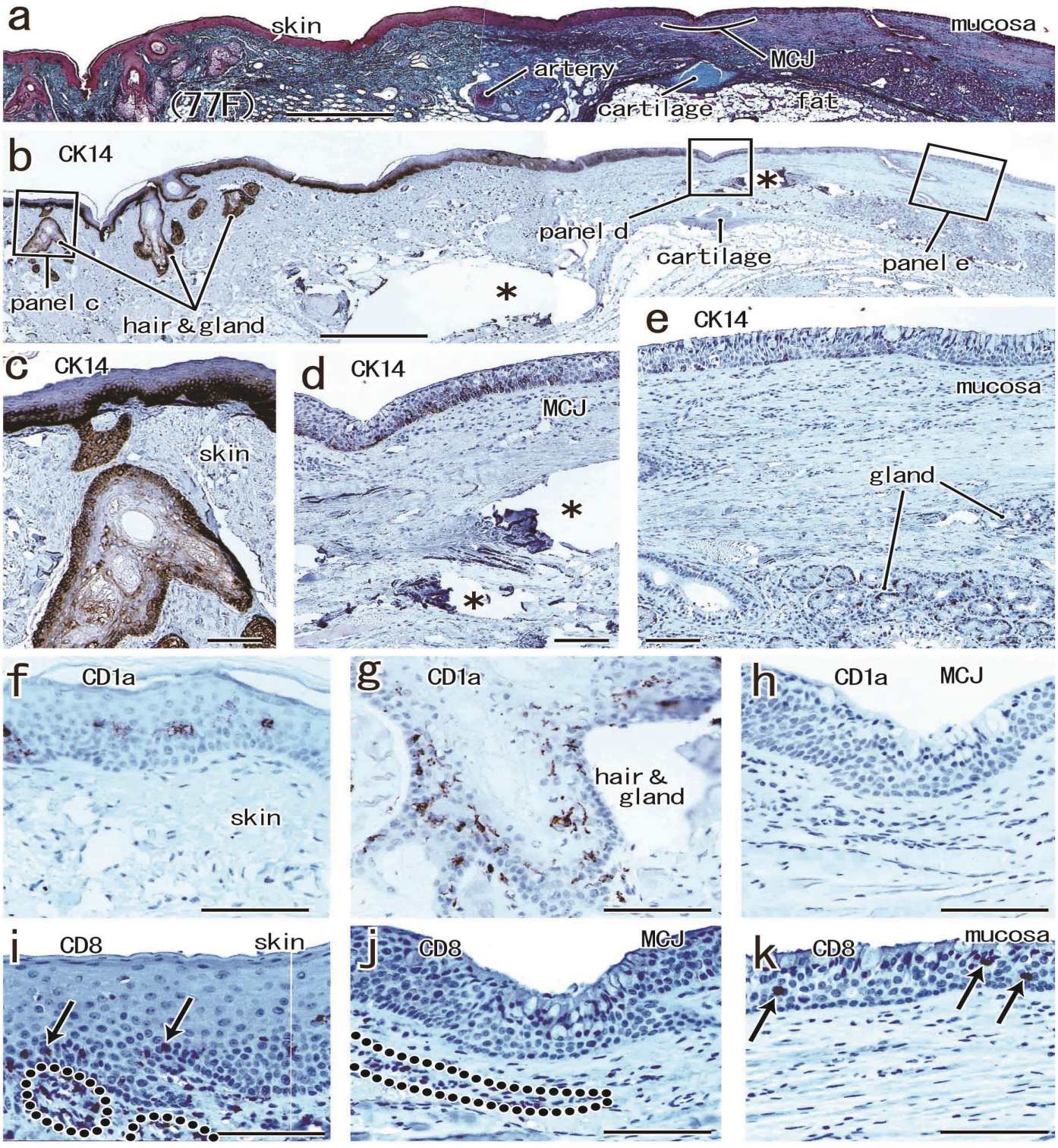
Figure 4. MCJ at the external nasal orifice of late-stage fetuses.



Annals of Dermatological Science (ISSN 2831-8129)

HE staining (panels a-f) and S100 immunohistochemistry (panel g and h). Panels a-d, a single frontal section from a 215-mm fetus; panels e-h, from a 334-mm fetus. Panels b-d (or panels f and h) are higher-magnification views of the squares in panel a (or panel e). Panel g, a section near panel a, shows the site indicated by a circle in a. Panels g and h show immunohistochemistry for S100 protein. The skin (panels b and f) contains abundant glands, hairs and striated muscle fibers of the nasalis muscle (NM). The mucocutaneous junction (MCJ) is covered by stratified squamous epithelium (panel d) and, beneath it, loose fibrous tissue is associated. The nasal mucosa comprises stratified columnar epithelium (panel c) or respiratory epithelium (columnar epithelium with cilia; panel h). Note the linear arrangement of nerves (dotted line in panel g) in the nasal subcutaneous tissue. The nasal skin and epithelium (specimen same as that in panel e, 334-mm fetus) are also shown in Fig. 1b, g and k. Scale bars, 1 mm in panels a, e and g; 0.1 mm in panels b-d, f and h.

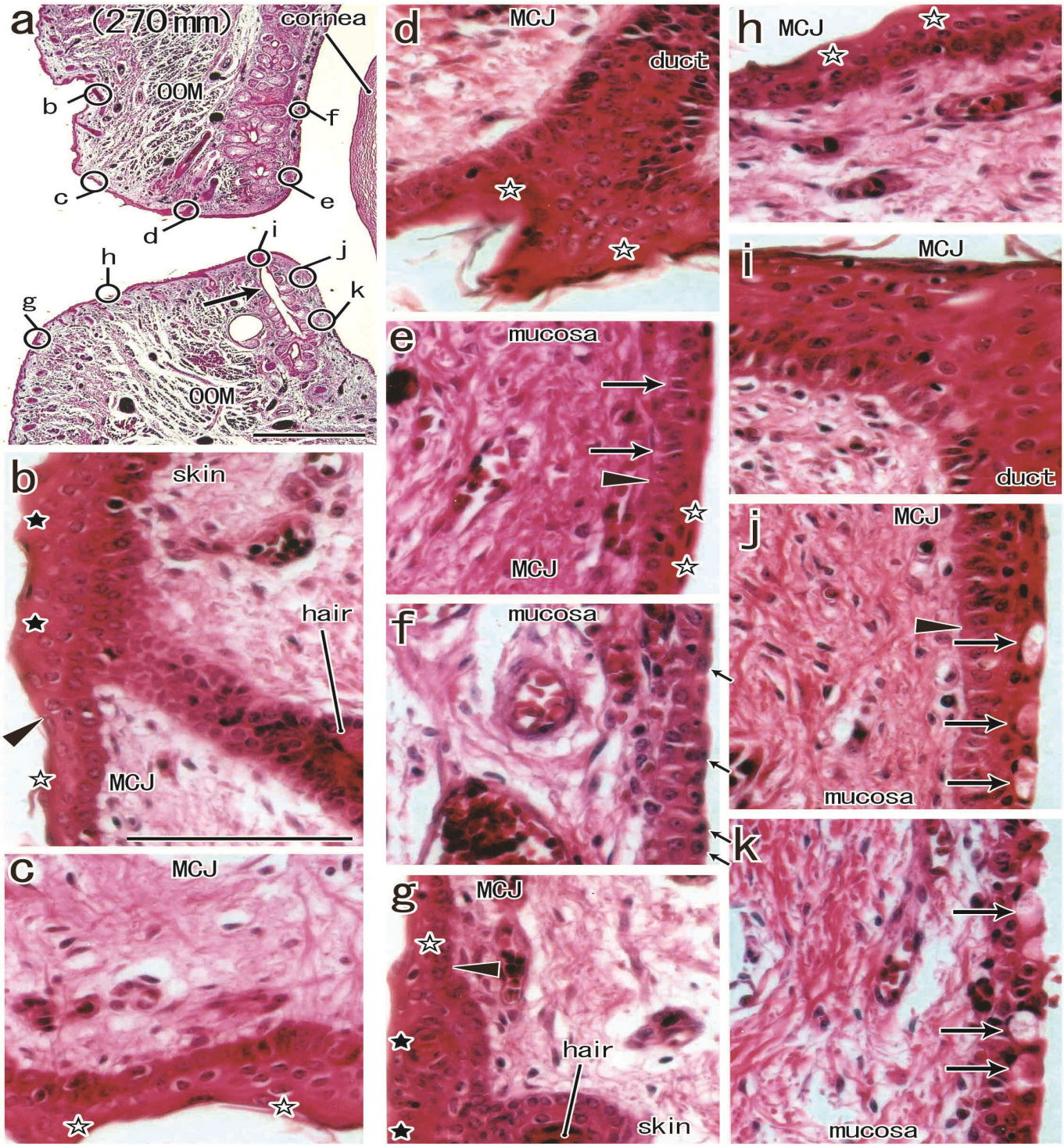
Figure 5. Reactivities for cytokeratin, CD1a and CD8 in the skin, MCJ and mucosa near the external nasal orifice of adult cadavers.



Annals of Dermatological Science (ISSN 2831-8129)

A 77-year-old woman. Panel a, elastica Masson staining; Panels b-e, immunohistochemistry for cytokeratin 14 (CK14); panels f-h, immuno-histochemistry for CD1a showing Langerhans cells; panels i-k, immuno-histochemistry for CD8 showing suppressor T lymphocytes). Panels a and b display adjacent sections and their left-hand margins corresponds a site almost 20 mm deep or further within the external orifice of the nose. The hairs and associated glands disappear at a site 20-21 mm from the orifice entrance, while the columnar epithelium with goblet cells appears at a site 35-36 mm from the orifice entrance. CK14 reactivity is strong in the basal part of the epidermis and weak or very weak in the MCJ and mucosa (panels c-e). Acinus cells beneath the mucosa express CK14 (panel e). Langerhans cells are sparsely distributed in the epidermis (panel f) and densely distributed in the hair follicles (panel g). The MCJ and mucosa do not contain Langerhans cells. Mononuclear cell infiltration (surrounded by dotted line in panels I and j) including CD8-positive T lymphocytes is evident beneath the epidermis and MCJ, but absent beneath the mucosa. Goblet cells are seen in the center of panel j. The epidermis and columnar epithelium contain CD8-positive cells (arrows in panels i and k). Asterisks in panels b and d indicate tissue damage during the histological procedure. Scale bars: 1 mm in panels a and b; 0.1 mm in panels c-k.

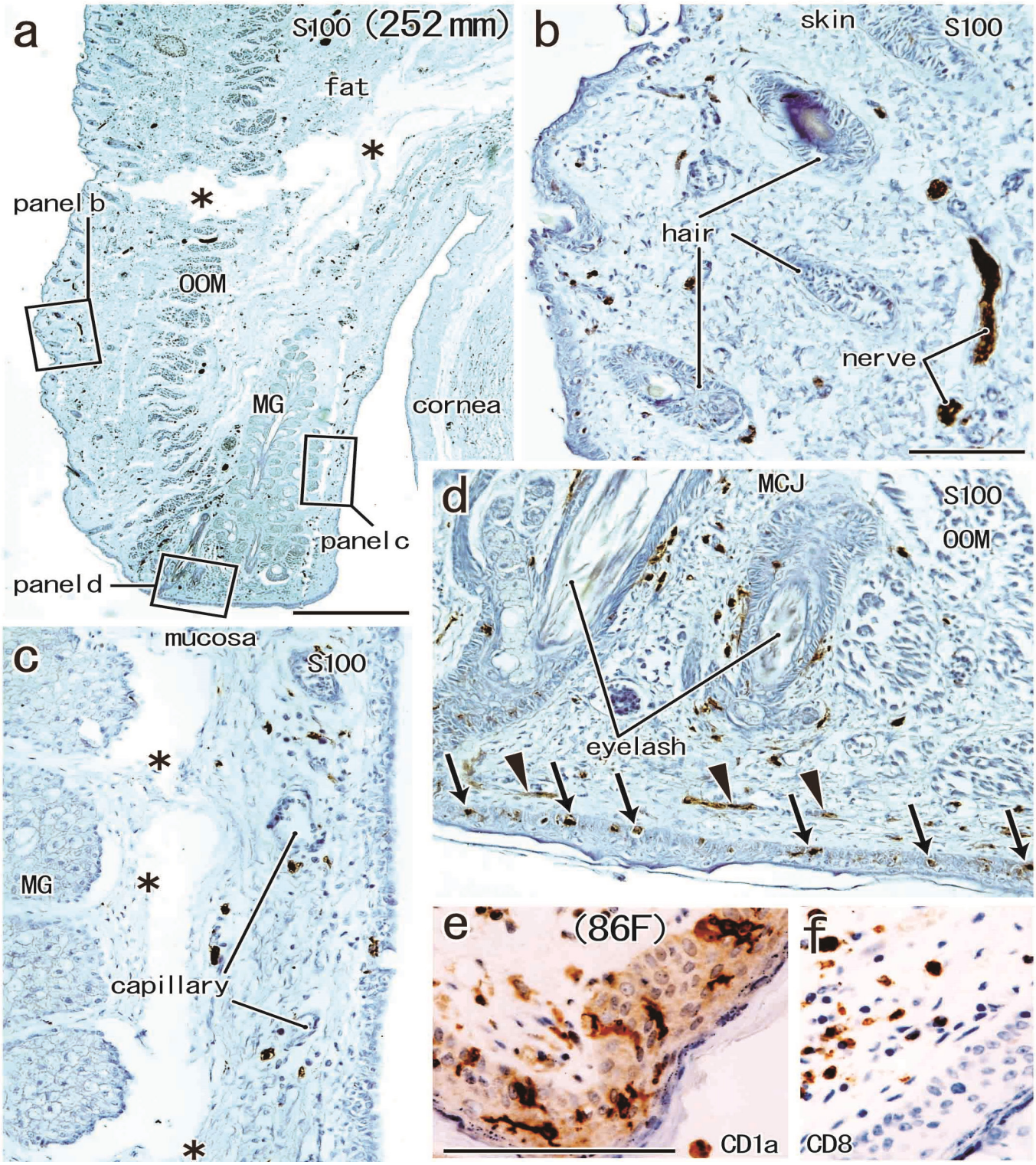
Figure 6. Identification of the skin-MCJ-mucosa in the upper and lower eyelids of a late-stage fetus (CRL 260 mm).



Annals of Dermatological Science (ISSN 2831-8129)

HE staining. Panel a displays the topographical anatomy: 10 circles are shown in panels b-k at higher magnification. In the upper lid, thick stratification of the epidermis (black stars in panel b) changes to a thin layer (open star) at a site indicated by the arrowhead (candidate skin-MCJ junction). The thin stratification of the epithelium continues to panels d and e (open stars). In the epithelium panel e, intercellular spaces (arrows) appear superior to a site indicated by the arrowhead (candidate MCJ-mucosa junction). Round nuclei (arrows in panel f) are arranged in line along the epithelial surface. In the lower lid, thick stratification (black stars) of the epidermis changes to a thin layer (open star; MCJ) at a site indicated by the arrowhead in panel g, and at a site indicated by the arrowhead in panel J, the MCJ connects to the stratified mucosa containing candidate goblet cells with vacuoles (arrows in panels j and k). Panels b-k were prepared at the same magnification. OOM, orbicularis oculi muscle. Scale bars: 1 mm in panel a; 0.1 mm in panel b.

Figure 7. Nerve distribution at the MCJ in the upper eyelid of a near-term fetus and immunoreactive cells in an elderly individual: immunohistochemistry for S100 protein, CD1a and CD8

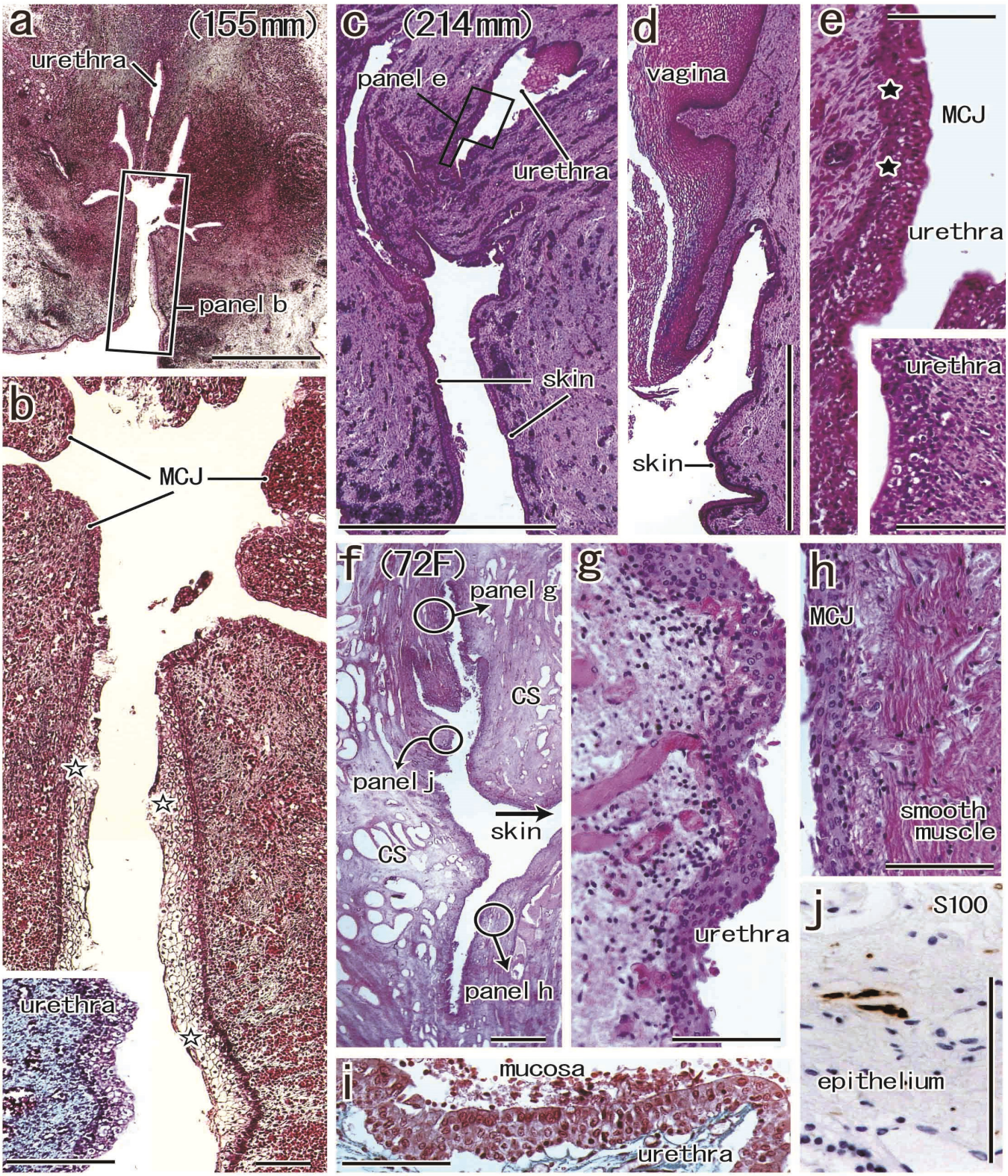


Panels a-d (immunohistochemistry for S100 protein) display a single sagittal section of the upper eyelid from a 252-mm fetus. Panels e and f

Annals of Dermatological Science (ISSN 2831-8129)

show immunohistochemistry for CD1a and CD8 at the MCJ of the upper lid in a specimen from an 86-year-old woman (same as shown in Fig. 3). Panels b-d (same magnification) are higher-magnification views of the squares in panel a. The nerve density is higher on the conjunctival side (panel c) than on the skin side (panel b). At the MCJ (panel d), a thin nerve runs along the anteroposterior axis (arrowheads), while corpuscle-like nerve terminals are scattered in the surface epithelium (arrows). Asterisks indicate tissue damage during the histological procedure. The MCJ and conjunctival mucosa contain abundant CD1a-positive Langerhans cells (panel e), but T-lymphocytes are restricted to the subcutaneous or submucosal tissue (panel f). OOM, orbicularis oculi muscle; MG, meibomian glands. Panels b-d or panels e and f were prepared at the same magnification (scale bars: 1 mm in panel a, 0.1 mm in panels b and e).

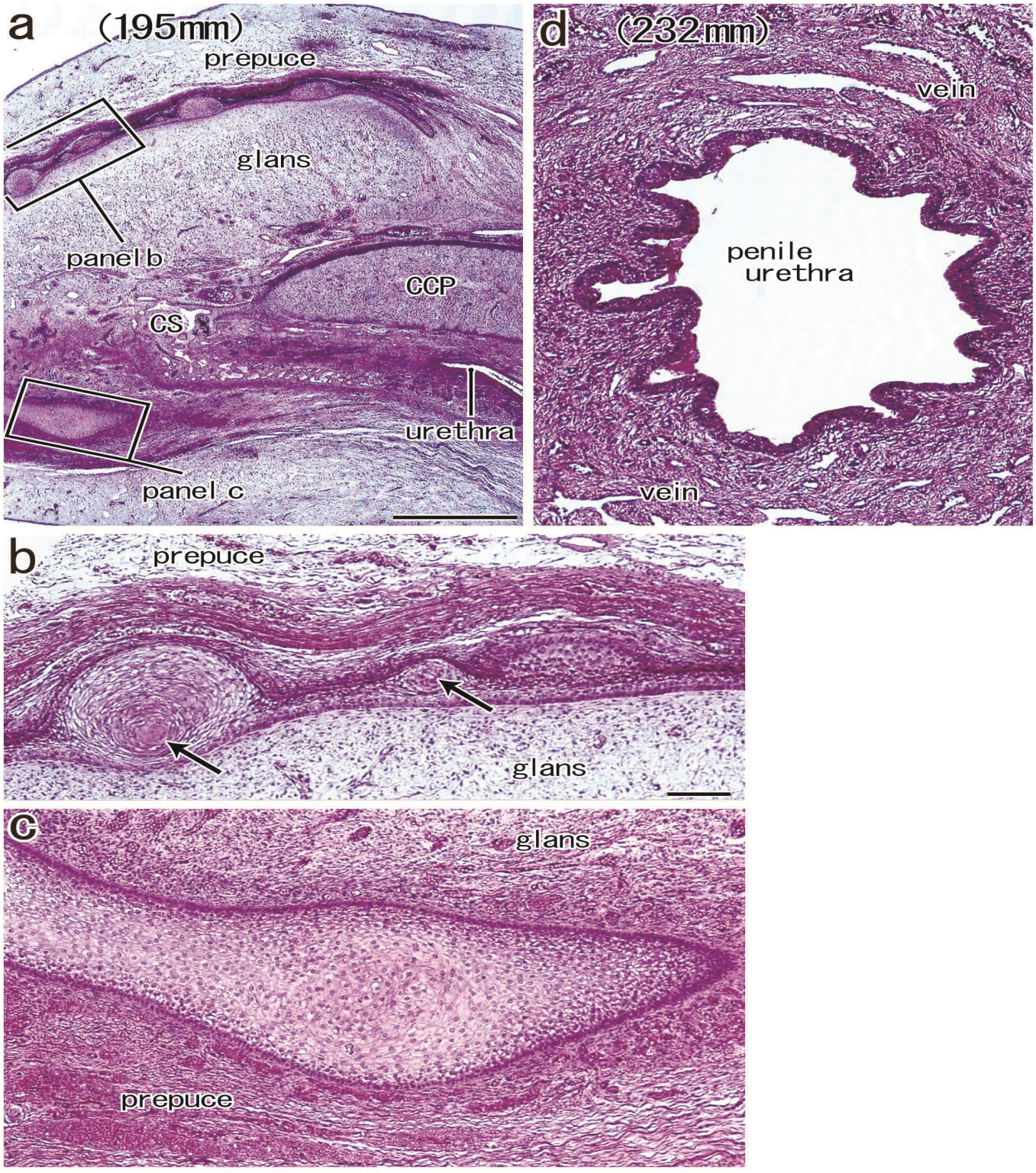
Figure 8. MCJ in the vulva: changes with age.



Annals of Dermatological Science (ISSN 2831-8129)

HE staining (panels a-e), elastica Masson staining (panels f-i) and S100 immunohistochemistry (panel j). Panels a and b, a 155-mm fetus; panels c-e, a 215-mm fetus; panels f-j, a specimen from a 72-year-old woman. Panels b and e are higher-magnification views of the square in panel a, respectively, and they contain inserts showing the urethral mucosa 1 mm distal to the orifice. Panel d, a plane 0.2 mm posterior to panel c, shows highly stratified squamous epithelium of the vagina. Panels g, h and j, corresponding to the circle in panel f, exhibit the urethral mucosa containing abundant veins (panel g) and smooth muscles (panel h) but few nerves (panel j). Panel i shows the distal urethral mucosa 5 mm distal to the orifice. Thick stratification (open stars in panel b) is evident at the approximation surfaces of the perineal epidermis in the early stage. A non-squamous epithelium with thick stratification (panels e, g and h) appears to correspond to the MCJ at the vulva. Scale bars: 1 mm in panel a, c, d and f; 0.1 mm in panels b, e, g, h, i and the insert in panel a.

Figure 9. Cornification filling the space between the prepuce and glans penis in a late-stage fetus.

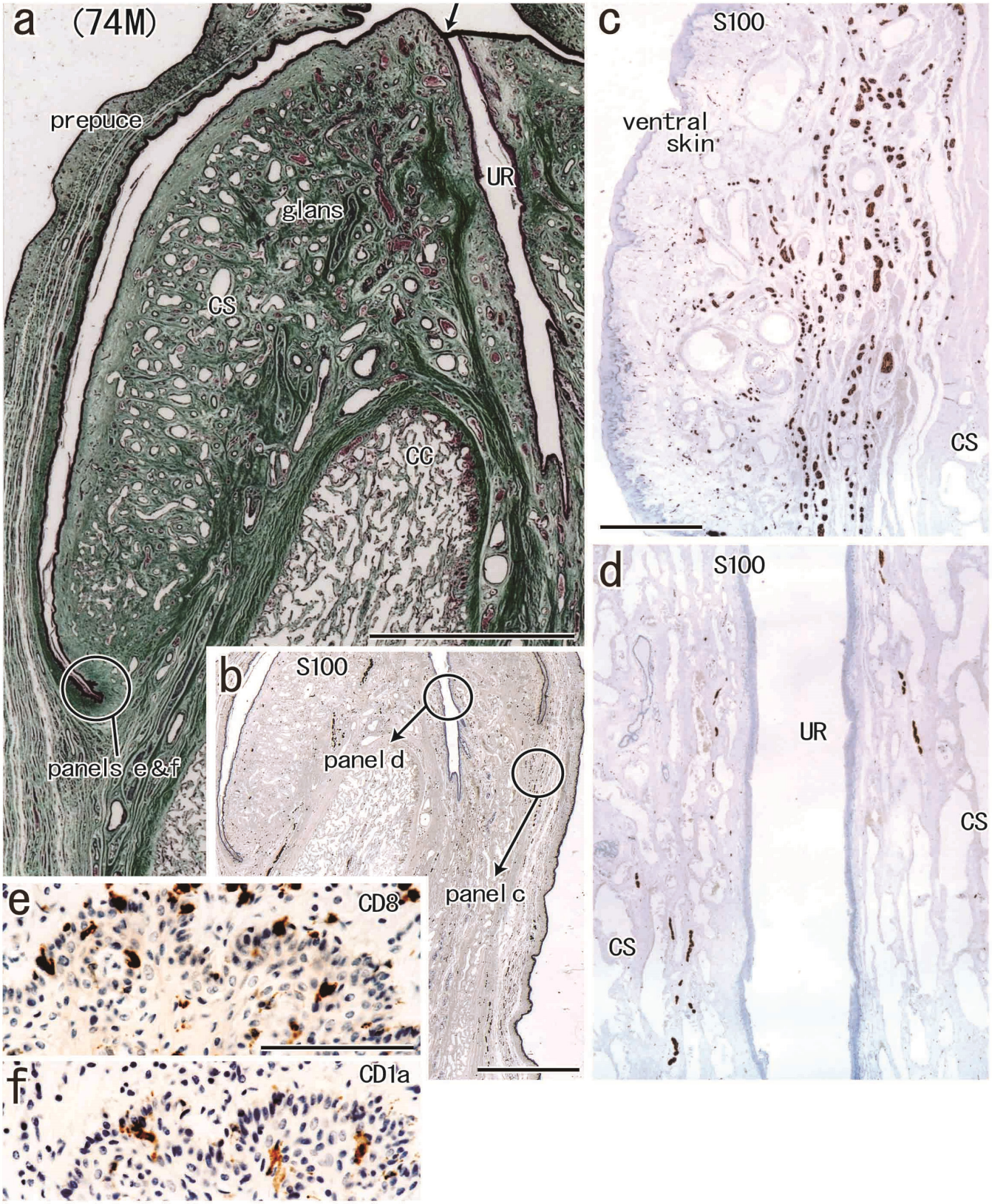


HE staining. Panels a-c display a 195-mm fetus (sagittal section), while panel d shows a 232-mm fetus (transverse section).

Annals of Dermatological Science (ISSN 2831-8129)

Panels b and c, higher- magnification views of the squares in panel a, showing thick cornification (high stratification) closing the space between the prepuce and glans penis. Epithelial pearl-like structures are evident in the cornification (arrows in panel b). At this stage, the urethral mucosa is pseudocolumnar and the lamina propria contains abundant veins (panel d). CCP, corpus cavernosum penis; CS, cavernous sinus. Panels b-d were prepared at the same magnification. Scale bars: 1 mm in panel a; 0.1 mm in panel b.

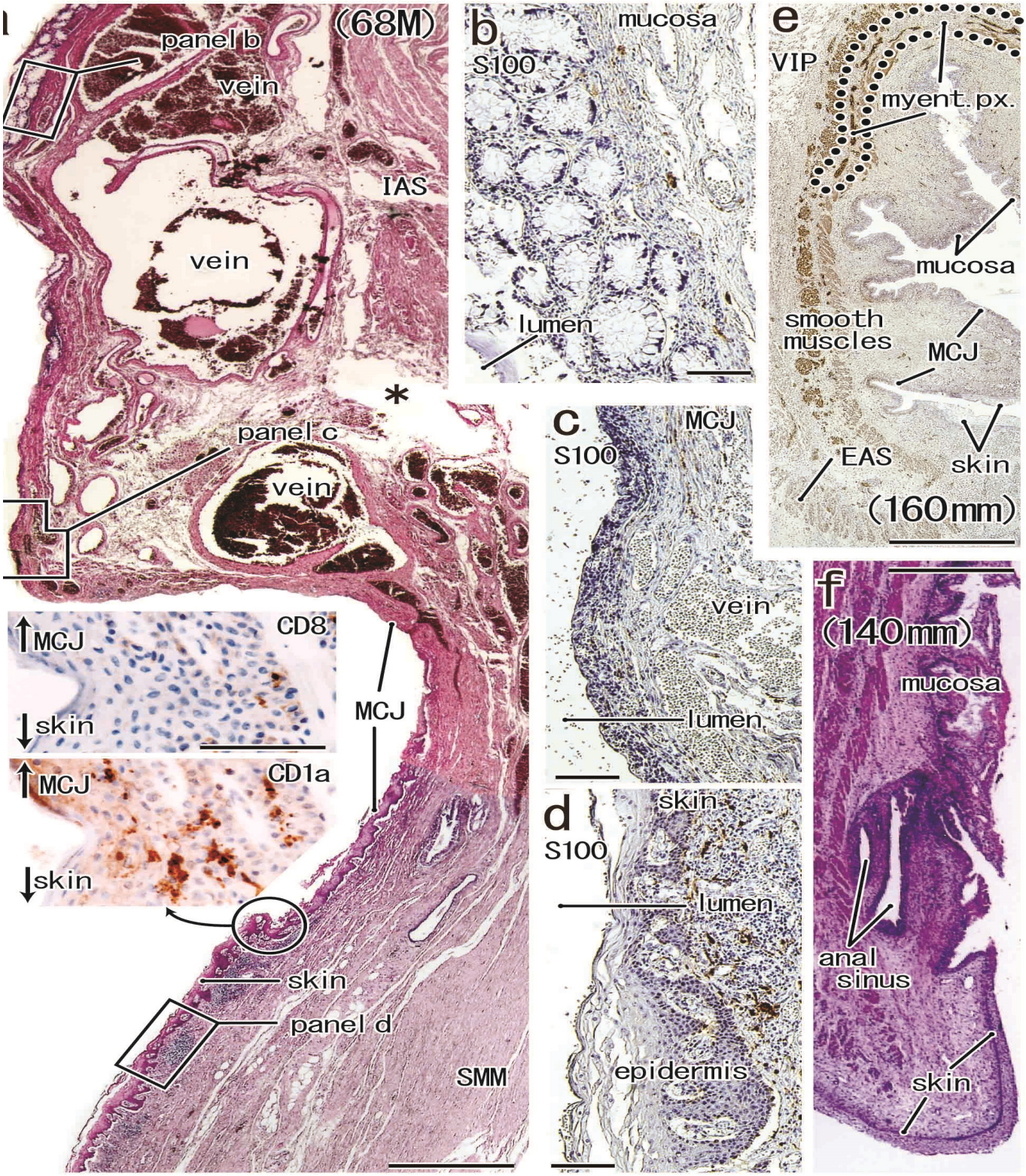
Figure 10. Skin of the prepuce and glans penis of a 75-year-old man.



Annals of Dermatological Science (ISSN 2831-8129)

Panel a, Masson trichrome; panels b-d, S100 protein immunohistochemistry; panel e, CD8 immunohistochemistry; panel f, CD1a immunohistochemistry. Panels a and b are adjacent sections. Arrow at the urethral orifice in panel A indicates an artifact (tissue fragment). Panels c and d are higher-magnification views of the circles in panel b, while panels e and f correspond to the circle at the lower angle of the prepuce in panel a. Abundant nerve twigs take highly tortuous courses beneath the penile skin (panel c) in contrast to only a few nerves along the urethra (UR; panel d). The penile skin contains many more CD8-positive lymphocytes than Langerhans cells (panels d and e). CS, cavernous sinus of the veins beneath the skin and mucosa. Panels c and d or panels e and f were prepared at the same magnification. Scale bars: 5 mm in panels a and b; 0.1 mm in panels c and e.

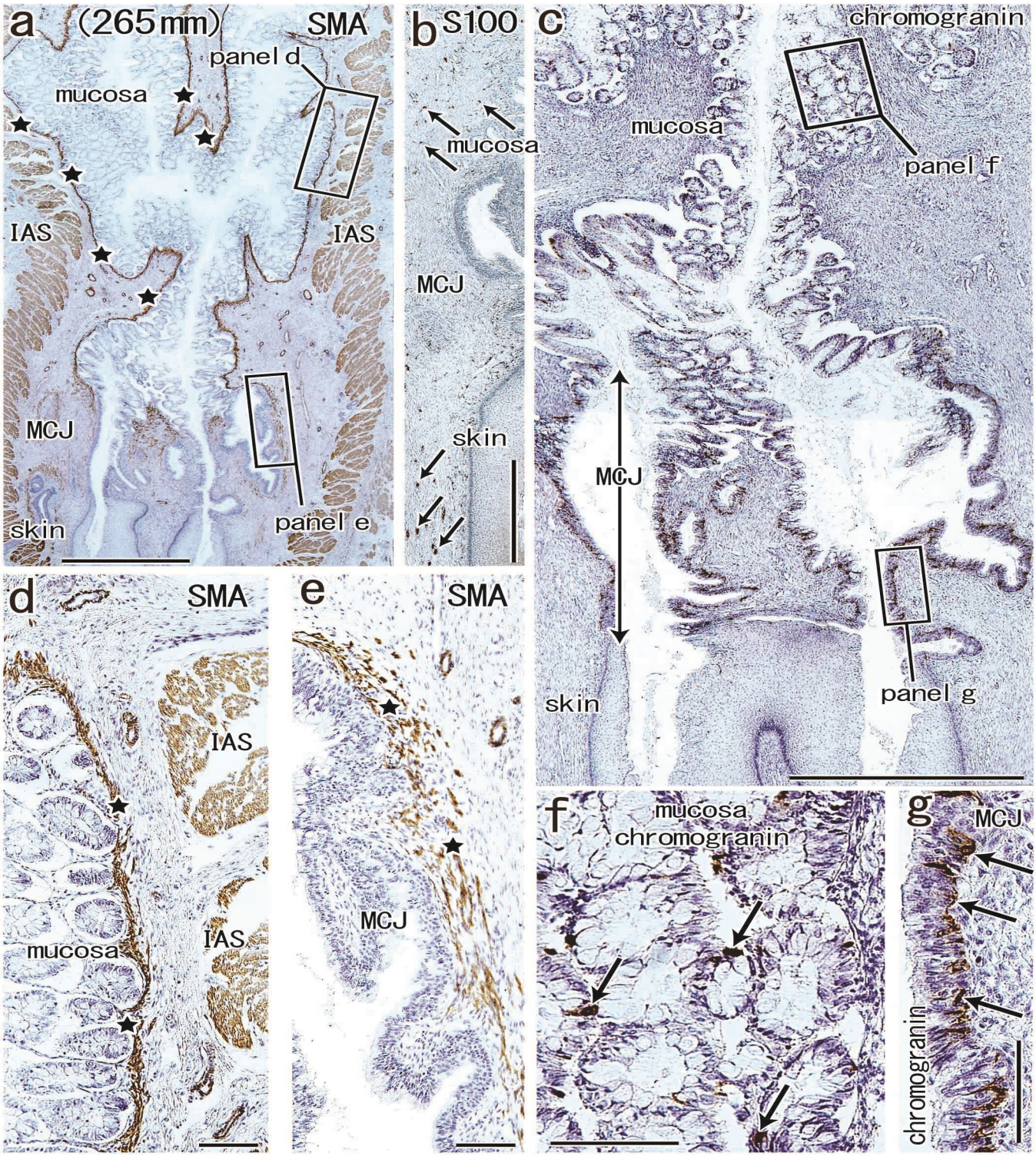
Figure 11. MCJ at the anal canal of an elderly individual and a late-stage fetus.



Annals of Dermatological Science (ISSN 2831-8129)

Panels a-d, longitudinal sections of the lateral anal wall of a 68-year-old man; panel e, frontal section of a 160-mm fetus. Panels b-d (immunohistochemistry for S100 protein) show higher-magnification views of the squares in panel a. In the elderly individual (panel a), a long MCJ (usually called the "anal transitional zone") extends between the columnar epithelium and skin epidermis. The epithelium contains abundant mononuclear cells (panel d). Panel e (immunohistochemistry for vasoactive intestinal polypeptide (VIP)) exhibits a myenteric nerve plexus extending beneath the mucosa. A non-specific reaction is seen in the two smooth muscle layers. Panel f displays the developing anal sinus (origin of the future MCJ epithelium) in a 140-mm fetus. Two inserts of panel a show that Langerhans cells predominate over CD8-positive lymphocytes in the skin. EAS, external anal sphincter (striated muscle); IAS, internal anal sphincter (smooth muscle); SMM, submucosal longitudinal smooth muscle (muscularis mucosae). Panels b-d were prepared at the same magnification (scale bars: 1 mm in panels a and e and an insert, 0.1 mm in panels b-d).

Figure 12. Anal submucosal muscle (muscularis mucosae) and chromogranin-positive cells at the MCJ of the anal canal in a 195-mm fetus.



Annals of Dermatological Science (ISSN 2831-8129)

Panels a, d and e, immunohistochemistry for smooth muscle actin (SMA); panel b, immunohistochemistry for S100 protein (S100); panels c, f and g, immunohistochemistry for chromogranin A. Panels d and e (or Panels f and g) are higher magnification views of squares in panel a (or panel c). The muscularis mucosae (stars) disperses to provide a thick but loose layer at MCJ (panel e). Panel B displays few or absent nerve beneath the MCJ in contrast to abundant nerves at the submucosal and subcutaneous area (arrows). Chromogranin A-positive neuroendocrine cells are few in the mucosa (panel f) but rich at the basal layer of the MCJ (panel g). scale bars: 1 mm in panels a-c, 0.1 mm in panels d-g.

DISCUSSION

We re-examined the morphology of the MCJ in humans to clarify similarities and differences among five sites (Tables 1-4) and, especially in fetuses, we considered what features might be site-specific (Table 5). In the eyelids, nasal orifice, urethral orifice and anus, the MCJ is a transitional area in which the skin epidermis connects to a non-squamous epithelium. Therein, the developing MCJ epithelium in fetuses was more or less similar to a stratified squamous epithelium rather than a columnar, cuboidal or pseudostratified columnar epithelium. Pseudostratified epithelium is known to show an intermediate morphology with active proliferation, differentiation and nuclear movement, and in embryos it covers various sites including the neural groove and canal [52]. The fetal MCJ we observed might correspond to a stage of development successive to the embryonic pseudostratified epithelium.

Although they are usually found intercalated within a simple columnar epithelium, goblet cells are interspersed within a stratified MCJ at the eyelid [2, 43] as well as the anal canal [45]. The present figures demonstrated not only their candidates (Figs. 1en and 6jk) but goblet cells at the stratified MCJ of the elderly nose (Fig. 5j). Notably, at the eye and anus, goblet cells are most likely to secret a very large and heavy O-glycosylated mucin MUC5AC [43, 45].

The nasal and male urethral orifices were transiently obliterated with cornification or hypertrophic keratinized cells of the skin. The oral mucosa also showed distinct hypertrophy in fetuses and the stratified squamous surface was continuous across the mouth. This continuity might explain the exceptionally short MCJ: the skin would suddenly lose the underlying dermal papillae. However, the mouth was not fused by any adhering cornification. Likewise, without cornification, the approximation surfaces of the eyelids in fetuses are tightly attached until 14-15 weeks of gestation (almost 100 mm CRL)[53, 54]. but blinking begins in utero [5]. Suckling movements also start in utero [55, 56] and adhesion of the mouth seems to be avoided.

The skin and MCJ generally contained abundant CD1a-positive Langerhans cells, while the lamina propria of the mucosa usually contained abundant CD8-positive suppressive T lymphocytes. At and near the MCJ epithelium, Langerhans cells seemed to constitute a limited subpopulation for receiving and presenting surface antigens. The skin and MCJ contained corpuscle-like nerve terminals along the wavy base of the epidermis, while free nerve ends were evident beneath the mucosa. However, the oral mucosa contains encapsulated nerve terminals [57] and a Merkel cell-neurite complex [58].

MCJ expansion was evident in the nasal orifice in specimens from elderly individuals. Such an expanded MCJ may occur as a result of stimulation by dry and/or cool air and is usually termed “squamous metaplasia” as a precursor tissue of squamous carcinoma [59]. Likewise, in the anal canal, elongation of the anal MCJ was most likely to occur along the supero-inferior axis with dilated hemorrhoid veins beneath the epithelium: this change may result from stimulation by hard feces.

The MCJ at the vulva and prepuce was long and wide even in fetuses, and had a specifically thin stratified epithelium. Although we suspected that the morphology might be influenced by age-related hormonal conditions, we had no opportunity to observe the histology in young adults. The vulva and prepuce are also characterized by strong and specific expression of CK7, as is the case in the urogenital tract (see the Introduction). Therefore, the MCJ might develop from the urethral mucosa. Despite having a very thick stratified squamous epithelium, the vagina also expresses CK7.

Study limitations

Because of delayed fixation and long-term preservation, immunohistochemistry of human fetal specimens often yielded inconsistent results, including absence of any reactivity. Moreover, in previous studies, the antibodies employed changed and differed year-by-year. This made it difficult to compare immunohistochemical results, especially for cytokeratin, among various research groups. A further study using specimens from a single well-fixed young cadaver will therefore be necessary for a comparison among the five MCJ sites.

Acknowledgment

We are grateful to the individuals who donated their bodies to Tokyo Dental College for research and education on human anatomy. We also express deep gratitude to the families who donated fetuses to Akita University School of Medicine.

Author Contributions

CRediT authorship contribution statement

Kei Kitamura: Conceptualization; data curation; formalanalysis; writing-original draft.

Yuki Sugiyama: Conceptualization; data curation;

formalanalysis; writing-original draft.

Kotoko Imai: Conceptu-alization; formal analysis; methodology; writing-originaldraft.

Tianyi Yang: For-mal analysis; project administration; validation; writing review and editing.

Ryo Sekiya: Conceptualization; investigation; methodol-ogy; supervision; writing-review and editing.

Kazuma Morita: Conceptualization; Data curation; methodol-ogy; supervision; writing-review and editing.

Gen Murakami: Formal analysis;investigation; supervision; writing-original draft; writing-review and editing.

Hitoshi Yamamoto: Data curation; investigation; visualization;writing-review and editing.

Shin-ichi Abe: Data curation; investigation; visualization;writing-review and editing

Declarations

Conflict of interest: No conflicts of interest declared.

Ethical approval: This study was conducted in accordance with the Declaration of Helsinki. The use of the study specimens was approved by the Ethics Committee of Tokyo Dental College (No. 922-2, 932-2).

REFERENCES

1. Fawcett DW (1994) Skin, In Bloom and Fawcett a textbook of histology. (12th edn) Chapman & Hall New, York: 525-554.

2. Knop E, Knop N, Zhivov A, Kraak R, Korb DR, et al. (2011) The lid wiper and muco-cutaneous junction anatomy of the human eyelid margins: an in vivo confocal and histological study. J Anat 218(4):449-461.

3. Tektaş OY, Yadav A, Garreis F, Schlötzer-Schrehardt U, Schicht M, et al. (2012) Characterization of the mucocutaneous junction of the human eyelid margin and meibomian glands with different biomarkers. Ann Anat 194(5):436-445.

4. Cho KH, Sugiyama Y, Watanabe G, Hirouchi H, Hayashi K, et al. (2024) Mentalis nerve branches supplying the lower lip revisited: a study using human fetuses and elderly donated cadavers. Surg Radiol Anat in press.

5. Cho KH, Honma K, Kim JH, Murakami G, Rodríguez-Vázquez JF, et al. (2024) Variations in thickness and muscle layer of the term upper eyelid and its clinical implication. Surg Radiol Anat in press.

6. Ming ME, Daryanani HA, Roberts LP, Baden HP, Kvedar JC (1994) Binding of keratin intermediate filaments (K10) to the cornified envelope in mouse epidermis: implications for barrier function. J Investig Dermatol Symp Proc 103(6):780-784.

7. Herrera-Imbroda B, Aragón IM, Hierro MI, Álvarez M, Alaminos M, et al. (2017) An immunohistochemical study of cytokeratins distribution of the human adult male and female urethra. Histol Histopathol 32:283-291.

8. Shen J, Isaacson D, Cao M, Sinclair A, Cunha GR, et al. (2018) Immunohistochemical expression analysis of the human fetal lower urogenital tract. Differentiation 103:100-119.

9. Fritsch H, Auer R, Hörmann R, Pechriggl E, Regauer S, et al. (2021) The development of the human vaginal fornix and the portio cervicis. Clin Anat 34(7):1059-1067.

10. Henry JJ, Charlebois TS, Grainger RM (1993) Differential expression of type II cytokeratin mRNA defines early developmental boundaries within the ectoderm, mesoderm and endoderm during chick development. Rouxs Arch Dev Biol 202(6):355–363.

11. Lungova V, Verheyden JM, Herriges J, Sun X, Thibeault SL (2015) Ontogeny of the mouse vocal fold epithelium. Dev Biol 399(2):263–282.

12. Moon WS, Cho BH, Hayashi S, Kim JH, Murakami G, et al. (2011) Cytokeratin-positive hepatocytes in the hilar region: an immunohistochemical study using livers from fetuses and elderly individuals. Ann Anat 193(3):224-230.

13. Hieda K, Hayashi S, Kim JH, Murakami G, Cho BH, et al. (2013) Spatial relationship between expression of cytokeratin-19 and that of connexin-43 in human fetal kidney. Anat Cell Biol 46(1):32-38.

14. Kim JH, Jin ZW, Murakami G, Cho BH (2016) Characterization of mesenchymal cells beneath cornification of the fetal epithelium and epidermis at the face: an immunohistochemical study using human fetal specimens. Anat Cell Biol 49(1):50-60.

15. Omine Y, Hinata N, Yamamoto M, Kasahara M, Matsunaga S, et al. (2015) Regional differences in the density of Langerhans cells, CD8-positive T lymphocytes and CD68-positive macrophages: a preliminary study using elderly donated cadavers. Anat Cell Biol 48(3):177-187.

Annals of Dermatological Science (ISSN 2831-8129)

16. Ramieri G, Panzica GC, Viglietti-Panzica C, Modica R, Springall DR, et al. (1992) Non-innervated Merkel cells and Merkel-neurite complexes in human oral mucosa revealed using antiserum to protein gene product 9.5. Arch Oral Biol 37(4):263-269.

17. WatanabeIS(2004)Ultrastructuresofmechanoreceptors in the oral mucosa. Anat Sci Int 79(2):55-61.

18. Lundblad L, Lundberg JM, Brodin E, Anggård A (1983) Origin and distribution of capsaicin-sensitive substance P-immunoreactive nerves in the nasal mucosa. Acta Otolaryngol 96(5-6):485-93.

19. Hauser-Kronberger C, Hacker GW, Franz P, Albegger K, Dietze O (1997) CGRP and substance P in intraepithelial neuronal structures of the human upper respiratory. Regul Pept 72(2-3):79-85.

20. Halata Z, Munger BL (1986) The neuroanatomical basis for the protopathic sensibility of the human glans penis. Brain Res 371(2):205-30.

21. García-Mesa Y, García-Piqueras J, Cobo R, Martín-Cruces J, Suazo I, et al. (2021) Sensory innervation of the human male prepuce: Meissner's corpuscles predominate. J Anat 239(4):892-902.

22. Li L, Li Z, Huo HS, Wang HZ, Wang LY (1992) Sensory nerve endings in the puborectalis and anal region of the fetus and newborn. Dis Colon Rectum 35(6):552-559.

23. Jang HS, Hinata N, Cho KH, Bando Y, Murakami G, et al. (2017) Nerves in the cavernous tissue of the glans penis: an immunohistochemical study using elderly donated cadavers. J Anat Soc India 66:91-96.

24. Yamamoto M, Hayashi S, Honkura Y, Hirano-Kawamoto A, Katori Y, et al. (2023) Nasal capsule ossification: A histological study using human foetuses to find an association between the foetus and adult morphologies of the nasal wall. J Anat 243(3):517-533.

25. Yamamoto M, Hirota Y, Watanabe G, Taniguchi S, Murakami G, et al. (2024) Development and growth of median structures in the human tongue: A histological study using human fetuses and adult cadavers. Anat Rec (Hoboken) 307(2):426-441.

26. Ishizuka S, Takahashi S, Kitamura K, Yang T, Abe S et al. (2024) Growth patterns of the facial muscles at the angle of month: a study using near-term human fetuses. J Anat in press.

27. Kim JH, Jin ZW, Shibata S, Yang JD, Murakami G, et al. Fetal development of human oral epithelial pearls with special reference to their stage-dependent changes in distribution. Cleft Palate Craniofac J 54(3):295-303.

28. Kim JH, Oka K, Jin ZW, Murakami G, Rodríguez-Vázquez JF, et al. (2017) Fetal Development of the Incisive Canal, Especially of the Delayed Closure Due to the Nasopalatine Duct: A Study Using Serial Sections of Human Fetuses. Anat Rec (Hoboken) 300(6):1093-1103.

29. Kim JH, Ishizuka S, Murakami G, Rodríguez-Vázquez JF. (2024) Striated muscles in the subcutaneous or submucosal tissue: a histological study using human fetuses and adult cadaveric specimens. Anat Cell Biol in press.

30. Kurokawa T, Hinata N, Sasaki H, Murakami G, Fujisawa M, et al. (2014) Perineal membrane: its relation to the levator ani and deep transverse perineal muscles, the composite fibers and nerve contents. Open J Obstet Gynecol 4:405-415.

31. Arakawa T, Murakami G, Ohtsuka A, Goto T, Teramoto T (2004) Variations in anal submucosal muscles in elderly Japanese subjects. Biomedical Research 25(1):45-52.

32. Arakawa T, Hwang SE, Kim JH, Wilting J, Rodríguez-Vázquez JF, et al. (2016) Fetal growth of the anal sinus and sphincters, especially in relation to anal anomalies. Int J Colorectal Dis 31(3):493-502.

33. Hieda K, Cho KH, Arakawa T, Fujimiya M, Murakami G, et al. (2013) Nerves in the intersphincteric space of the human anal canal with special reference to their continuation to the enteric nerve plexus of the rectum. Clin Anat 26(7):843-854.

34. Ishiyama G, Hinata N, Kinugasa Y, Murakami G, Fujimiya M (2014) Nerves supplying the internal anal sphincter: an immunohistochemical study using donated elderly cadavers. Surg Radiol Anat 36(10):1033-1042.

35. Kinugasa Y, Arakawa T, Murakami G, Fujimiya M, Sugihara K (2014) Nerve supply to the internal anal sphincter differs from that to the distal rectum: an immunohistochemical study of cadavers. Int J Colorectal Dis 29(4):429-443.

36. Motohashi O, Suzuki M, Shida N, Umezawa K, Ohtoh T, et al. (1995) Subarachnoid haemorrhage induced proliferation of leptomeningeal cells and deposition of extracellular matrices in the arachnoid granulations and subarachnoid space. Immunhistochemical study. Acta Neurochir (Wien) 136(1-2):88-91.

37. Hayashi T, Kumasaka T, Mitani K, Yao T, Suda K, et al. (2010) Loss of heterozygosity on tuberous sclerosis complex genes in multifocal micronodular pneumocyte hyperplasia. Mod Pathol 23(9):1251-60.

38. Claeys S, Cuvelier C, Van Cauwenberge P (1996) Immunohistochemical analyses of the lymphoepithelium in human nasopharyngeal associated lymphoid tissue (NALT): preliminary results. Acta Otolaryngol Suppl 523:38-39

39. Park HS, Francis KP, Yu J, Cleary PP (2003) Membranous cells in nasal-associated lymphoid tissue: a portal of entry for the respiratory mucosal pathogen group A streptococcus. J Immunol 171(5):2532-2537.

40. Jahnsen FL, Farstad IN, Aanesen JP, Brandtzaeg P (1998) Phenotypic distribution of T cells in human nasal mucosa differs from that in the gut. Am J Respir Cell Mol Biol 18(3):392-401.

41. Jahnsen FL, Gran E, Haye R, Brandtzaeg P (2004) Human nasal mucosa contains antigen-presenting cells of strikingly different functional phenotypes. Am J Respir Cell Mol Biol 30(1):31-37.

42. Ríos JD, Forde K, Diebold Y, Lightman J, Zieske JD, et al. (2000) Development of conjunctival goblet cells and their neuroreceptor subtype expression. Ophthalmol Vis Sci 41(8):2127-2137.

43. Gipson IK (2016) Goblet cells of the conjunctiva: A review of recent findings. Prog Retin Eye Res 54:49-63.

44. Brandtzaeg P (1997) Mucosal immunity in the female genital tract. J Reprod Immunol 36(1-2):23-50.

45. Muranaka F, Nakajima T, Iwaya M, Ishii K, Higuchi K, et al. (2018) A Comparative Immunohistochemical Study of Anal Canal Epithelium in Humans and Swine, Focusing on the Anal Transitional Zone Epithelium and the Anal Glands. Anat Rec (Hoboken) 301(5):796-805.

46. Hörsch D, Fink T, Büchler M, Weihe E (1993) Regional specificities in the distribution, chemical phenotypes, and coexistence patterns of neuropeptide containing nerve fibres in the human anal canal. J Comp Neurol 335(3):381-401.

47. Hörsch D, Fink T, Göke B, Arnold R, Büchler M, et al. (1994) Distribution and chemical phenotypes of neuroendocrine cells in the human anal canal. Regul Pept 54(2-3):527-542.

48. Shia J, Tang LH, Weiser MR, Brenner B, Adsay NV, et al. (2008) Is nonsmall cell type high-grade neuroendocrine carcinoma of the tubular gastrointestinal tract a distinct disease entity? Am J Surg Pathol 32(5):719-731.

49. Madahian S, Judelson R, Zhu X, Meng X, Dresser K, et al. (2021) CD56 expression in basaloid anal squamous cell carcinoma - A potential diagnostic pitfall. Ann Diagn Pathol 53:151758. https://doi.org/10.1016/j.anndiagpath.2021.151758

50. Ramalingam P, Hart WR, Goldblum JR (2001) Cytokeratin subset immunostaining in rectal adenocarcinoma and normal anal glands. Arch Pathol Lab Med 125(8):1074-1077.

51. Yaghoobi M, Le Gouvello S, Aloulou N, Duprez-Dutreuil C, Walker F, et al. (2011) FoxP3 overexpression and CD1a+ and CD3+ depletion in anal tissue as possible mechanisms for increased risk of human papillomavirus-related anal carcinoma in HIV infection. Colorectal Dis 13(7):768-773.

52. Ferreira MA, Despin-Guitard E, Duarte F, Degond P, Theveneau E (2019) Interkinetic nuclear movements promote apical expansion in pseudostratified epithelia at the expense of apicobasal elongation. PLoS Comput Biol 15(12):e1007171. https://doi.org/10.1371/journal.pcbi.1007171

53. Sevel D (1988) A reappraisal of the development of the eyelids. Eye (Lond) 2 (2):123-9.

54. Tawfik HA, Abdulhafez MH, Fouad YA, Dutton JJ (2016) Embryologic and Fetal Development of the Human Eyelid. Ophthalmic Plast Reconstr Surg 32(6):407-414.

55. Hepper PG, Shahidullah S, White R (1911) Handedness in the human fetus. Neuropsychologia 29(11):1107-1111.

56. Kim TH, Lee JJ, Chung SH, Lee HH, Lee KH, et al. (2010)

Efficacy of assessment in fetal behaviour by four dimensional ultrasonography. J Obstet Gynaecol 30(5):439-443.

57. Tachibana T, Ishizeki K, Sakakura, Y (1987) Distinct types of encapsulated sensory corpuscles in the oral mucosa of the dog: immunohistochemical and electron microscopic studies. Anat Rec 217(1):90-98.

58. Cobo R, García-Piqueras J, Cobo J, Vega JA (2021) The human cutaneous sensory corpuscles: an update. J Clin Med 10(2):227

59. Kawahara T, Miyaguchi M, Sakai S, Uda H, Kuwabara H, et al. (1994) Immunohistological study of dendritic cells and macrophages in sino-nasal lesions--distributions in metaplastic squamous epithelium and squamous cell carcinoma. Nihon Jibiinkoka Gakkai Kaiho 97(2):240-246.

60. Barrett AW, Morgan M, Nwaeze G, Kramer G, Berkovitz BK (2005) The differentiation profile of the epithelium of the human lip. Arch Oral Biol 50:431-438.

61. Kasper M, Stosiek P (1990) The expression of vimentin in epithelial cells from human nasal mucosa. Eur Arch Otorhinolaryngol. 248(1):53-56.

62. Schwerer MJ, Kraft K, Baczako K, Maier H (2001) Coexpression of cytokeratins typical for columnar and squamous differentiation in sinonasal inverted papillomas. Am J Clin Pathol 115(5):747-754.

63. Levy R, Czernobilsky B, Geiger B (1991) Cytokeratin polypeptide expression in a cloacogenic carcinoma and in the normal anal canal epithelium. Virchows Arch A Pathol Anat Histopathol 418(5):447-455.

64. Williams GR, Talbot IC, Northover JM, Leigh IM (1995) Keratin expression in the normal anal canal. Histopathology 26(1):39-44.

65. Mechtersheimer G, Brandt I, Möller P (1986) Differences in marker expression among branched histiocytic cells in T-cell areas of the lymphoreticular system and among their epidermis- and mucosa-associated equivalents. Cell Tissue Res 244(3):471-478.

66. Cruchley AT, Williams DM, Farthing PM, Lesch CA, Squier CA (1989) Regional variation in Langerhans cell distribution and density in normal human oral mucosa determined using monoclonal antibodies against CD1, HLADR, HLADQ and HLADP. J Oral Pathol Med 18(9):510-516.

67. Reinartz SM, van Tongeren J, van Egmond D, de Groot EJ, Fokkens WJ, et al. (2016) Dendritic Cell Subsets in Oral Mucosa of Allergic and Healthy Subjects. PLoS One 11(5):e0154409. https://doi.org/10.1371/journal.pone.0154409

68. Yoshimi R, Takamura H, Takasaki K, Kumagami H (1993) Immunohistologic study of the nasal mucosa with reference to Langerhans cells. Nihon Jibiinkoka Gakkai Kaiho 96(8):1252-1257.

69. Graeme-Cook F, Bhan AK, Harris NL (1993) Immunohistochemical characterization of intraepithelial and subepithelial mononuclear cells of the upper airways. Am J Pathol 143(5):1416-1422.

70. Takasaki K (1996) Immunohistologic study of the nasal mucosa with reference to Langerhans cells. Nihon Jibiinkoka Gakkai Kaiho 99(5):695-699.

71. Morinaka S, Nakamura H (2000) Inflammatory cells in nasal mucosa and nasal polyps. Auris Nasus Larynx 27(1):59-64.

72. Karosi T, Csomor P, Hegyi Z, Sziklai I (2013) The presence of CD209 expressing dendritic cells correlates with biofilm positivity in chronic rhinosinusitis with nasal polyposis. European archives of oto-rhino-laryngology 270(9):2455-2463.

73. Hingorani M, Metz D, Lightman SL (1997) Characterisation of the normal conjunctival leukocyte population. Exp Eye Res 64(6):905-912.

74. Morelli AE, Ronchetti RD, Secchi AD, Cufré MA, Paredes A, et al. (1992) Assessment by planimetry of Langerhans' cell density in penile epithelium with human papillomavirus infection: changes observed after topical treatment. J Urol 147(5):1268-1273.

75. Qin Q, Zheng XY, Wang YY, Shen HF, Sun F, et al. (2009) Langerhans' cell density and degree of keratinization in foreskins of Chinese preschool boys and adults. Int Urol Nephrol 41(4):747-753.

76. Gervaz E, Dauge-Geffroy MD, Sobhani I, Vissuzaine C, Mignon M, et al. (1995) Quantitative analysis of the immune cells in the anal mucosa. Pathol Res Pract 191(11):1067-1071.

Annals of Dermatological Science (ISSN 2831-8129)

77. Hilliges M, Astbäck J, Wang L, Arvidson K, Johansson O (1996) Protein gene product 9.5-immunoreactive nerves and cells in human oral mucosa. Anat Rec 245(4):621-632.

78. Zhao C, Tao Z, Xiao J, Zhao S, Qiao J (1995) An immunocytochemical study on relations between mast cell and peptidergic terminals in nasal mucosa of chronic rhinitis patients. Chin Med J (Engl) 108(8):606-609.

79. Hinata N, Murakami G, Abe S, Honda M, Isoyama T, et al. (2012) Detailed histological investigation of the female urethra: application to radical cystectomy. J Urol 187(2):451-456.